

Representative roughness height of submerged vegetation

Cheng, Nian-Sheng

2011

Cheng, N. S. (2011). Representative roughness height of submerged vegetation. *Water resources research*, 47(8).

<https://hdl.handle.net/10356/83700>

<https://doi.org/10.1029/2011WR010590>

© 2011 American Geophysical Union. This paper was published in *Water Resources Research* and is made available as an electronic reprint (preprint) with permission of American Geophysical Union. The paper can be found at: [DOI: <http://dx.doi.org/10.1029/2011WR010590>]. One print or electronic copy may be made for personal use only. Systematic or multiple reproduction, distribution to multiple locations via electronic or other means, duplication of any material in this paper for a fee or for commercial purposes, or modification of the content of the paper is prohibited and is subject to penalties under law.

Downloaded on 30 Jan 2023 09:57:20 SGT

Representative roughness height of submerged vegetation

Nian-Sheng Cheng¹

Received 22 February 2011; revised 11 June 2011; accepted 24 June 2011; published 18 August 2011.

[1] Roughness length scale is important in the evaluation of resistance caused by submerged vegetation in open channel flows. By transforming the concept of hydraulic radius, a representative roughness height is proposed in this study for quantifying effect of submerged vegetation on flow resistance in the surface layer. The proposed roughness height is characterized by its proportionality to both stem diameter and vegetation concentration and performs better than other length scales in collapsing resistance data collected under a wide range of vegetation conditions. An approach is then developed for estimate of the average flow velocity and thus resistance coefficients for both cases of rigid and flexible vegetation. Comparisons are also made between the present study and other four formulas available in the literature. This study also shows that all the formulas, if simplified for some simple conditions, can be unified in a general form.

Citation: Cheng, N.-S. (2011), Representative roughness height of submerged vegetation, *Water Resour. Res.*, 47, W08517, doi:10.1029/2011WR010590.

1. Introduction

[2] Considerable studies have been conducted in the past decades to explore, experimentally and analytically, effects of submerged vegetation on characteristics of open channel flows [e.g., *Huthoff et al.*, 2007; *Kouwen et al.*, 1969; *Meijer and van Velzen*, 1999; *Murphy et al.*, 2007]. However, how to describe vegetation-affected velocity profiles and evaluate relevant flow resistance and sediment transport rates remain challenging. In this study, we attempt to formulate representative roughness height of submerged vegetation in open channel flows.

[3] If compared with fully rough flows over immobile sediment beds, vegetated channel flows seem more complex. This could be exemplified by comparing roughness length scales. For a typical sediment bed without bedforms, it is well known that sediment size can be used to reasonably characterize boundary roughness length, which resembles sand-roughened pipes investigated by *Nikuradse* [1933]. In comparison, for vegetated channel flows, roughness size varies with vegetation configurations, and thus cannot be simply quantified using a single geometrical dimension such as vegetation height, spacing between stems, and stem diameter. Different considerations have been presented in the literature. For example, *Kouwen et al.* [1969] early recommended use of the vegetation height in the evaluation of vegetation resistance. They reported that for particular vegetation configuration, the ratio of the average velocity to shear velocity is closely related to the ratio of flow depth to vegetation height, in a logarithmic function similar to that applied for rough pipe flows,

$$\frac{U}{u_*} = a_1 + a_2 \ln\left(\frac{H}{h_v}\right), \quad (1)$$

¹School of Civil and Environmental Engineering, Nanyang Technological University, Singapore.

where U is the cross-sectional average velocity, u_* is the shear velocity, H is the flow depth, h_v is the vegetation height, and a_1 and a_2 are constants. Equation (1) suggests that the vegetation height be considered as an equivalent roughness height. However, no universal values are available for a_1 and a_2 , both varying with vegetation density and flexibility. Moreover, *Kouwen et al.* [1969] made no division between the flows above and inside the vegetation layer, in spite of the fact that they are characterized by different velocity and length scales.

[4] In considering similarities associated with the surface layer above vegetation, *Huthoff et al.* [2007] reported that the stem spacing, in comparison to vegetation height and stem diameter, could provide the best fit to experimental data. With scaling arguments that interpret Manning equation for rough channel flows [*Gioia and Bombardelli*, 2002], *Huthoff et al.* [2007] scaled the average velocity in the surface layer in the power law form,

$$\frac{U_s}{\sqrt{gh_s S}} \sim \left(\frac{h_s}{k}\right)^{1/6}, \quad (2)$$

where U_s is the average flow velocity in the surface layer (see Figure 1), h_s is the surface layer thickness, S is the energy slope, g is the gravitational acceleration and k is an equivalent roughness height that scales with other variables,

$$k \sim \frac{(C_D d)^3}{(s + d)^2}, \quad (3)$$

where C_D is the stem drag coefficient, d is the stem diameter and s is the stem spacing. If the number of stems per unit bed area is N , and the vegetation concentration is λ , then $(s + d)^2 \sim 1/N$, and $N = 4\lambda/(\pi d^2)$ for cylindrical stems. With these considerations, k can be further scaled as

$$k \sim \frac{4}{\pi} C_D^3 \lambda d. \quad (4)$$

Equation (4) shows that k varies in the order of λd if C_D can be approximated as a constant close to unity.

[5] Alternatively, the roughness height could be also evaluated by applying the logarithmic velocity profile to the surface layer [Baptist *et al.*, 2007; Liu *et al.*, 2008; Nepf and Vivoni, 2000],

$$\frac{u}{\sqrt{gh_s S}} = \frac{1}{\kappa} \ln\left(\frac{y - \Delta y}{y_o}\right), \quad (5)$$

where y is measured upward from the edge of vegetation, Δy is the zero-plane displacement, κ is the von Karman constant and y_o is the hydrodynamic roughness length. For example, Baptist *et al.* [2007] proposed that

$$y_o = L \left(1 - \exp\left(-\frac{h_v}{L}\right)\right) \exp\left(-\kappa \sqrt{\frac{40L}{h_s}} \left(1 + \frac{L}{h_s}\right)\right), \quad (6)$$

where $L = [\pi d h_s / (80 \lambda)]^{0.5}$. If assuming that the power law and logarithmic function applied above are equivalent, as demonstrated in open channel hydraulics, one may expect that y_o and k are comparable. This will be discussed further later in this paper.

[6] From the abovementioned studies, the following inferences could be made. First, the vegetation height h_v is an important parameter to quantify vegetation dimension, but it should not be taken as a representative length scale to describe vegetation roughness height. Second, considering different scales of the flow in the surface and vegetation layer (see Figure 1), it may be improper to define a single roughness length applicable to the entire bulk flow.

[7] This study aims to propose a representative roughness height for the surface layer, and then develop an approach to evaluation of bulk flow velocity and thus resistance coefficient (e.g., Manning and Chezy coefficient). Only simulated vegetation stems are considered, including rigid cylindrical rods and flexible film strips.

2. Conceptual Consideration

[8] The idea presented here is developed by transforming the concept of hydraulic radius. For pipe and channel flows, the hydraulic radius is defined as the ratio of cross-sectional area to wetted perimeter of the flow domain. In other words, the hydraulic radius can be understood as a length scale of the cross-sectional area, which is measured with respect to a unit length of the boundary. If considered in a three-dimensional space, the hydraulic radius can be also taken as a measure of the length scale of the fluid volume per

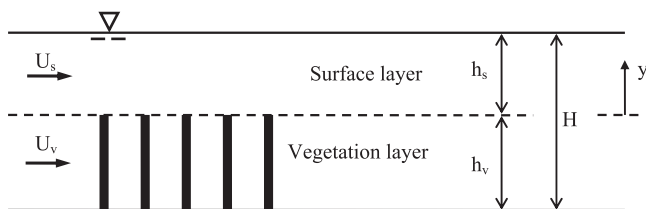


Figure 1. Vegetated open channel flow comprising surface and vegetation layer. U_v is the average velocity of the flow through stems.

unit boundary area. In the following, the three-dimensional explanation is extended to vegetated open channel flows.

[9] Here, we are concerned with vegetation simulated with rigid, cylindrical stems. It is assumed that (1) the configuration of vegetation is described by the stem diameter d and vegetation concentration λ (defined as the fraction of the bed area occupied by stems), (2) the volume of vegetation zone per unit bed area is measured as $1 \times h_v$, where h_v is the vegetation height, and (3) the bed friction is negligible. With λ and d , the total number of stems per unit bed area can be calculated as $N = \lambda / (\pi d^2 / 4)$.

[10] Then, we separate the total volume of the vegetation layer per unit bed area into two different components, vegetation-occupied volume, $\Phi_v (= \lambda h_v)$, and fluid-occupied volume, $\Phi_f [= (1 - \lambda) h_v]$. Note that the ratio of Φ_v to the total volume, $\Phi_v + \Phi_f$, defines the volumetric fraction of the vegetation, which is equal to λ . For this three-dimensional configuration, the hydraulic radius for the vegetation layer may be defined as the ratio of Φ_f to the wetted boundary area, A_v , i.e., the total wetted surface area of all stems. Such definitions have been used to evaluate flow resistance related to porous media [Cheng, 2003; Cheng *et al.*, 2008]. However, to better quantify the vegetation-induced form drag, A_v should be replaced with the frontal area of the stems, the latter being the area of the stems projected on a plane normal to the flow direction. This yields an effective wetted area, i.e., $A_v = N h_v d = 4 \lambda h_v / (\pi d)$. Being associated with vegetation-induced drag, A_v can also be understood as a counterpart of the boundary area for pipe and channel flows. Finally, the vegetation-related hydraulic radius is defined as

$$r_v = \frac{\Phi_f}{A_v} = \frac{(1 - \lambda) h_v}{4 \lambda h_v / (\pi d)} = \frac{\pi (1 - \lambda)}{4 \lambda} d. \quad (7)$$

This hydraulic radius provides a length scale for measuring the size of the fluid-occupied volume, Φ_f , with respect to the frontal area of stems, A_v . In a recent study [Cheng and Nguyen, 2011], we successfully applied the vegetation hydraulic radius to the evaluation of resistance induced by emergent vegetation in open channel flows.

[11] Similar to $A_v [= 4 \lambda h_v / (\pi d)]$ for the vegetation-occupied volume, the frontal area for the fluid-occupied volume can be evaluated as $A_f = 4(1 - \lambda) h_v / (\pi d)$. However, it should be mentioned that A_f is not the actual frontal area, and it is evaluated by imagining that Φ_f be filled up with stems as in Φ_v . To quantify how rough the stems are with respect to the fluid-occupied volume, we may define a length scale, k_v , as Φ_v / A_f , i.e.,

$$k_v = \frac{\Phi_v}{A_f} = \frac{\lambda h_v}{4(1 - \lambda) h_v / (\pi d)} = \frac{\pi \lambda}{4(1 - \lambda)} d. \quad (8)$$

Both r_v and k_v provide length scales in the sense of hydrodynamics. Like the hydraulic radius defined for other flows, r_v given in equation (7) signifies how spacious the flow domain is in the presence of boundary resistance (i.e., vegetation stems) for vegetated channel flows. In contrast, k_v given in equation (8) denotes the dimension of the vegetation-induced blockage with respect to the flow.

[12] Therefore, as a reasonable measure, k_v could be taken as the representative length scale to describe the size

of stem-induced roughness. Equation (8) shows that k_v is proportional to the vegetation concentration and stem diameter. If λ is constant, k_v would be in the order of d , which resembles the sediment size, i.e., roughness length scale for rough flows over a sediment bed. In section 4, it is shown that this roughness height, when normalized with the flow depth in the surface layer, performs well in collapsing resistance data collected with a wide range of vegetation configurations.

3. Data Collection

3.1. Experiments

[13] The experiments were carried out in a tilting rectangular flume, 12 m long, 0.3 m wide and 0.45 m deep, with almost the same setup as that described by *Cheng and Nguyen* [2011]. Flow discharges were measured using a built-in electromagnetic flowmeter with a standard deviation of 0.1–7.5%. The channel slopes were calculated from longitudinal flow depth variations, which were measured using a point gauge accurate to 0.1 mm while water in the flume remained stationary. The vegetation zone, 9.6 m long and 0.3 m wide, was simulated with rigid, circular cylindrical rods arranged in a staggered pattern. Three kinds of rods were used, with the same height ($h_v = 100$ mm) and different diameters ($d = 3.2, 6.6, \text{ and } 8.3$ mm). The resulted vegetation density λ varied from 0.43 to 11.90%. For each test, the flow depth was measured at five stations to ensure the achievement of uniform flow, and the flow velocity profile was measured at the centerline of the flume using a laser Doppler velocimetry. The data collected from 23 runs of experiments are listed in Table 1.

3.2. Other Data Sources

[14] In addition to the experiments conducted in the present study, the data reported in previous studies for submerged vegetation are also collected for subsequent analyses and comparisons. The previous data comprise 10

sources for the case of rigid vegetation and 6 for the case of flexible vegetation. The relevant information is summarized in Table 2. The large sets of data were contributed by *Shimizu et al.* [1991], *Meijer and van Velzen* [1999] [also see *Baptist*, 2005], *Stone and Shen* [2002] [also see *Stone*, 1997], and *Murphy et al.* [2007]. It is noted that various materials, including cylindrical rods, film strips and real plants, were used to simulate vegetation, and experiments were conducted in different sizes of flumes, e.g., the flume length ranging from 4.3 m [*Liu et al.*, 2008] to over 100 m [*Meijer and van Velzen*, 1999]. The configuration of vegetation also varied, with stems or strips being arranged in staggered pattern [e.g., *Dunn et al.*, 1996; *Kouwen et al.*, 1969; *Stone and Shen*, 2002], in linear pattern [e.g., *Kubrak et al.*, 2008; *Nezu and Sanjou*, 2008; *Shimizu et al.*, 1991; *Yan*, 2008], or even randomly [*Murphy et al.*, 2007].

[15] Altogether, 277 sets of data were gathered from the previous studies for the case of rigid vegetation and 103 sets of data for the case of flexible vegetation. A compilation of the data is provided in Appendix A, in terms of eight variables, i.e., channel width (B), flow depth (H), energy slope (S), discharge (Q), stem diameter or strip width (d), vegetation height (h_v), concentration (λ) and number of stems or strips per unit area (N).

3.3. Preprocessing of Data

[16] Noting that the data were collected from different sources or under different flow and vegetation conditions, some preprocessing should be conducted prior to comparison and analysis. For example, some experimental measurements could be subject to strong sidewall effect if the aspect ratio of a channel is not large. Similarly, bed effect could be also considerable for vegetation that is low or sparse or when the bed is covered with sand [*Cheng and Nguyen*, 2011]. To avoid such uncertainties, a general procedure is developed here for conducting sidewall and also bed corrections.

Table 1. Experimental Data Collected in the Present Study

Run	Discharge Q ($\text{m}^3 \text{s}^{-1}$)	Channel Width B (m)	Flow Depth H (m)	Energy Slope S	Vegetation Density λ (%)	Stem Diameter d (m)	Vegetation Height h_v (m)	Number of Stems per Unit Area N (m^{-2})
A30-15	0.0076	0.3	0.15	0.004	1.73	0.0032	0.1	2221
A30-17	0.0111	0.3	0.17	0.004	1.73	0.0032	0.1	2221
A30-20	0.0152	0.3	0.20	0.004	1.73	0.0032	0.1	2221
A60-13	0.0099	0.3	0.13	0.004	0.43	0.0032	0.1	556
A60-15	0.0128	0.3	0.15	0.004	0.43	0.0032	0.1	556
A60-17	0.0161	0.3	0.17	0.004	0.43	0.0032	0.1	556
A60-20	0.0205	0.3	0.20	0.004	0.43	0.0032	0.1	556
B30-13	0.0038	0.3	0.13	0.004	7.69	0.0066	0.1	2221
B30-15	0.0059	0.3	0.15	0.004	7.69	0.0066	0.1	2221
B30-17	0.0079	0.3	0.17	0.004	7.69	0.0066	0.1	2221
B30-20	0.0095	0.3	0.2	0.004	7.69	0.0066	0.1	2221
B60-13	0.0062	0.3	0.13	0.004	1.92	0.0066	0.1	556
B60-15	0.0096	0.3	0.15	0.004	1.92	0.0066	0.1	556
B60-17	0.0123	0.3	0.17	0.004	1.92	0.0066	0.1	556
B60-20	0.0161	0.3	0.20	0.004	1.92	0.0066	0.1	556
C30-13	0.0030	0.3	0.13	0.004	11.90	0.0083	0.1	2221
C30-15	0.0046	0.3	0.15	0.004	11.90	0.0083	0.1	2221
C30-17	0.0072	0.3	0.17	0.004	11.90	0.0083	0.1	2221
C30-20	0.0114	0.3	0.20	0.004	11.90	0.0083	0.1	2221
C60-13	0.0059	0.3	0.13	0.004	2.98	0.0083	0.1	556
C60-15	0.0079	0.3	0.15	0.004	2.98	0.0083	0.1	556
C60-17	0.0116	0.3	0.17	0.004	2.98	0.0083	0.1	556
C60-20	0.0154	0.3	0.20	0.004	2.98	0.0083	0.1	556

3.3.1. Sidewall Correction for Surface Layer

[17] Sidewalls affect the flow to different degree in the surface and vegetation layer. In the vegetation layer, the flow is largely subject to vegetation drag, the latter being much greater than bed and sidewall friction. However, in the surface layer, sidewall effect could be relatively significant, in particular, when the aspect ratio of the surface layer is not large, e.g., $B/h_s < 5$.

[18] Here, the procedure proposed for wall correction is similar to that developed by *Vanoni and Brooks* [1957]. First, work out the Reynolds number and friction factor using parameters related to the surface layer, i.e.,

$$Re_s = \frac{4U_s r_s}{\nu}, \quad (9)$$

$$f_s = 8 \frac{g r_s S}{U_s^2}, \quad (10)$$

where $r_s = Bh_s/(B + 2h_s)$. Then, the flow depth in the surface layer is modified as

$$h_{sm} = h_s \left(1 - \frac{f_w r_s}{0.5B f_s} \right), \quad (11)$$

where f_w is the sidewall friction factor and can be evaluated using the following empirical formula [*Cheng and Nguyen*, 2011],

$$f_w = 31 \left[\ln \left(\frac{1.3 Re_s}{f_s} \right) \right]^{-2.7}. \quad (12)$$

3.3.2. Bed and Sidewall Correction for Vegetation Layer

[19] In the vegetation layer, although the vegetation drag is usually dominant in comparison to bed and sidewall friction, bed and sidewall corrections are still necessary for certain cases. Such an approach has been presented by *Cheng and Nguyen* [2011] to modify the vegetation hydraulic radius for the case of emergent vegetation. Their results demonstrated that the bed correction appears necessary for the case of sand-covered bed. For the case of submerged vegetation, the average velocity in the vegetation layer is unknown so iteration is needed for implementing the correction procedure. However, computations with the data summarized in Table 2 show that unlike the correction made for the surface layer, the correction for the vegetation layer can be ignored for most of the cases considered because it has negligible effect on the final results presented in section 4.

[20] From the cases considered in this study and the information presented by *Cheng and Nguyen* [2011], it follows that corrections are considered significant only for (1) low aspect ratios, e.g., $B/h_s < 5$, for the surface layer, and (2) low vegetation densities, e.g., $\lambda < 10\%$, or sand-covered beds for the vegetation layer.

3.3.3. Uncertainties in Energy Slope Measurements

[21] Among various measured variables, the energy slope could be highly subject to uncertainties. In the previous studies, two different approaches have been applied to obtain energy slopes. Most of the slopes were derived from measured free surface slopes for uniform flows. The others were estimated from measured Reynolds shear stress profiles in the surface layer. *Murphy et al.* [2007] calculated energy slope from the gradient of the Reynolds shear stress in the vertical direction, while *Nezu and Sanjou* [2008] and

Table 2. Summary of Experiments Conducted by Previous Investigators^a

Investigator	Vegetation Zone		Vegetation Configuration				Flow Condition	Number of Runs	
	Width (m)	Length (m)	Stem Diameter d (mm)	Stem Height h_v (m)	Concentration λ (%)	Stem Shape			Pattern
<i>Rigid Vegetation</i>									
<i>Shimizu et al.</i> [1991]	0.5	6	1	0.041	0.44–0.79	cylindrical	linear	uniform	20
	0.4	6	1.5	0.046					8
<i>Dunn et al.</i> [1996]	0.91	2.44	6.35	0.118	0.14–1.23	cylindrical	staggered	uniform	12
<i>Meijer</i> [1998] [see <i>Baptist</i> , 2005]	3	20.5	8	0.45–1.5	0.32–1.29	cylindrical		nonuniform	48
<i>Stone and Shen</i> [2002]	0.45	11	3.18–12.7	0.124	0.55–6.10	cylindrical	staggered	uniform	128
<i>Poggi et al.</i> [2004]	0.9	9	4	0.12	0.08–1.35	cylindrical	linear	nonuniform	5
<i>Murphy et al.</i> [2007]	0.38		6.4	0.07; 0.14	1.18–3.77	cylindrical	random	nonuniform	24
<i>Liu et al.</i> [2008]	0.3	3	6.35	0.076	0.31–1.57	cylindrical	linear; staggered	uniform	9
<i>Nezu and Sanjou</i> [2008]	0.4	9	8	0.05		flat strip	linear	uniform	9
<i>Yan</i> [2008]	0.42	8	6	0.06	1.41–5.66	cylindrical	linear	uniform	12
<i>Yang</i> [2008]	0.45	6	2	0.035	0.44	cylindrical	staggered	uniform	2
Present study	0.3	9.6	3.2–8.3	0.1	0.43–11.90	cylindrical	staggered	uniform	23
<i>Flexible Vegetation</i>									
<i>Kouwen et al.</i> [1969]	0.61		5	0.05–0.1	9.82	flat strip	staggered	uniform	27
<i>Dunn et al.</i> [1996]	0.91		6.35	0.097–0.161	0.14–1.23	cylindrical	staggered	uniform	6
<i>Jarvela</i> [2003]	1.1	6	2.8–3	0.155–0.295	0.36–7.39	(wheat; sedge)		nonuniform	12
<i>Yang</i> [2008]	0.45	6	2	0.023–0.034	0.44	flat strip	staggered	uniform	5
<i>Kubrak et al.</i> [2008]	0.58	3	0.7; 0.95	0.131–0.164	0.13–0.54	cylindrical	linear	uniform	25
<i>Okamoto and Nezu</i> [2010]	0.40	10	8	0.03–0.1	4.78	flat strip	linear	uniform	28

^aFor flat strips, d is taken as stem width. For flexible vegetation, h_v is taken as deflected height, and λ is calculated as $\pi N d^2 / 4$, where N is the number of stems per unit bed area.

Poggi *et al.* [2004] estimated the slope or shear velocity from Reynolds shear stresses measured at the edge of vegetation stems. Such estimates would require that the flow depth of the surface layer is large enough so that the linear distribution of the Reynolds shear stress is clearly observed. As shown in the subsequent analysis (see Figure 4), a few data points (including five from *Murphy et al.* [2007] and three from *Nezu and Sanjou* [2008]) that deviate clearly from the main trend of the data could be due to low flow depth (e.g., $h_s < 5$ cm) in the surface layer. The diverging points are excluded for examining the main data trend as shown in Figure 4, but still used for comparisons with predictions in Figure 5.

3.3.4. Equivalent Concentration of Vegetation Simulated by Film Strips

[22] For the case of film strips, the strip width is taken as an equivalent stem diameter, which yields the same projected area in the flow direction. Then, the equivalent concentration is computed as $\pi Nd^2/4$, where d is the strip width and N is the number of stems per unit bed area.

4. Analyses and Comparisons

4.1. Variations of Friction Factor With Relative Roughness Height

[23] With the preprocessed data for the case of rigid vegetation, some possible friction factor relationships are examined here. First, the friction factor is defined simply using cross-sectional flow parameters, i.e.,

$$f = \frac{8grS}{U^2}, \tag{13}$$

where $U [= Q/(BH)]$ is the average flow velocity, $r [= BH/(B + 2H)]$ is the hydraulic radius, Q is the flow discharge, and B is the channel width. Correspondingly, the relative roughness height is defined as h_v/r . Figure 2 shows that the relationship of f and h_v/r is unclear. This may imply that it is improper to use h_v as an equivalent roughness height in the description of vegetation effects.

[24] Second, we only consider the upper surface layer by noting distinct characteristics of the two layers. Using the surface layer thickness h_s in place of r and the average surface layer velocity U_s in place of U , the friction factor is expressed as

$$f_s = \frac{8gh_sS}{U_s^2}, \tag{14}$$

where subscript s denotes the surface layer. Similarly, the relative roughness height is taken as h_v/h_s . Figure 3 shows that the relationship between f_s and h_v/h_s is again indistinct. In addition, we also plotted a graph (not included here) of $8gr_sS/U_s^2$ against h_v/r_s , where r_s is the hydraulic radius of the surface layer, displaying the data points in a scattering pattern very similar to Figure 3.

[25] Next, the proposed roughness height k_v (i.e., equation (8)) is used to revise the relative roughness height as k_v/h_s . The relationship of f_s and k_v/h_s is plotted with the same data in Figure 4. It shows that this relationship becomes much clearer than those plotted in Figures 2 and 3, in spite of a few deviating data points that include those reported by *Liu et al.* [2008], and also those with small values of h_s from *Murphy et al.* [2007] and *Nezu and Sanjou*

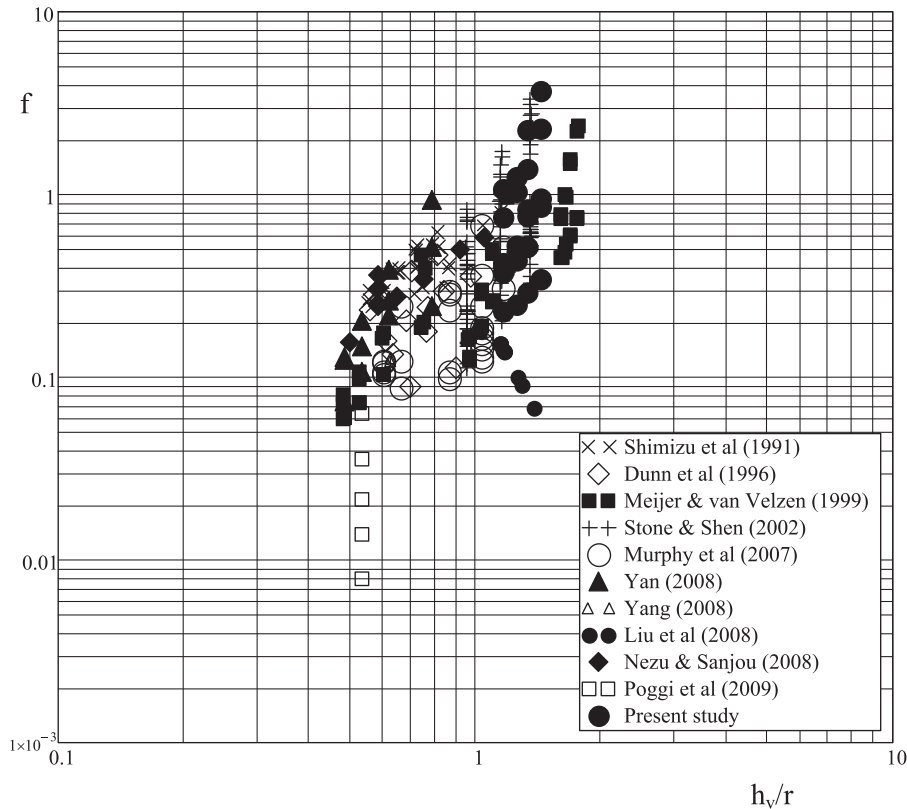


Figure 2. Relationship of $f [= 8grS/U^2]$ and h_v/r .

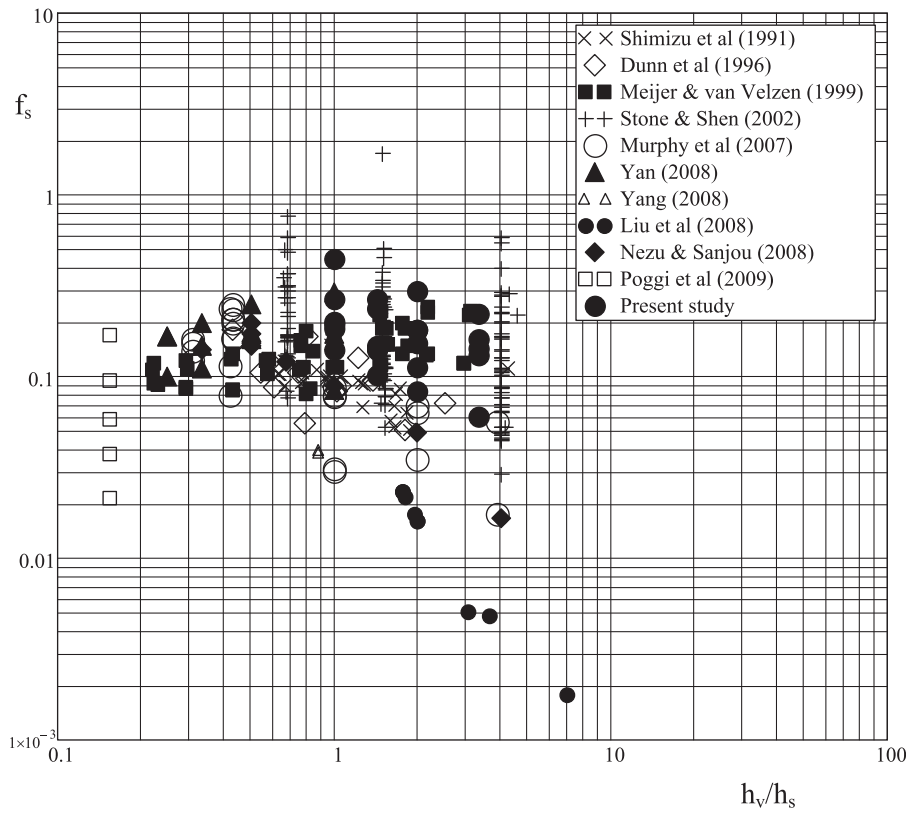


Figure 3. Relationship of $f_s [= 8gh_sS/U_s^2]$ and h_v/h_s .

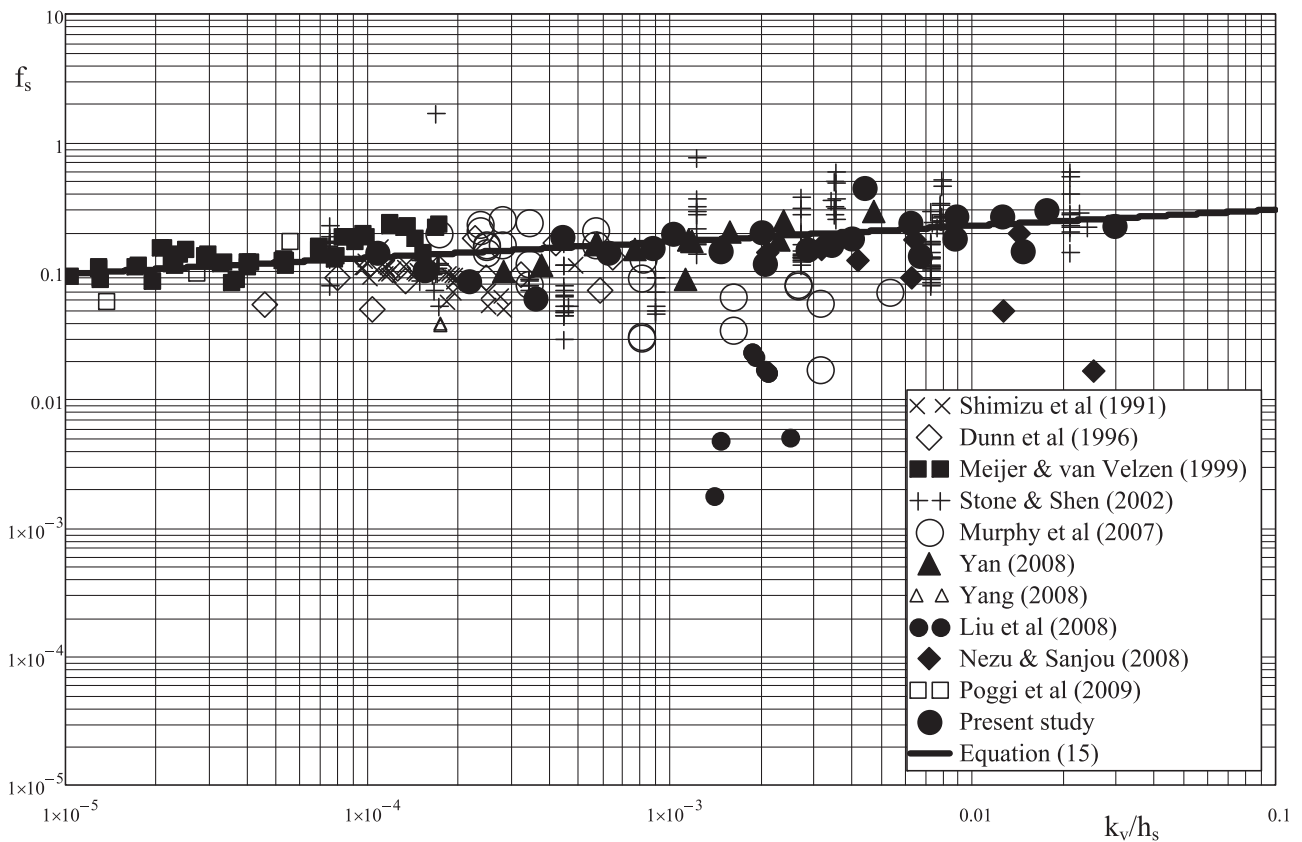


Figure 4. Relationship of $f_s [= 8gh_sS/U_s^2]$ and k_v/h_s .

[2008] (as mentioned in section 3.3.3). Additional computations also indicate that if using the modified flow depth of the surface layer (as given in equation (11)) in plotting Figure 4, the degree of scattering can be slightly reduced while the general data trend remains. This further suggests that it is the use of k_v that is helpful to clarify the friction factor relationship. As an approximation, the general data trend displayed in Figure 4 is fitted using the following function,

$$f_s = \alpha \left(\frac{k_v}{h_s} \right)^\beta, \quad (15)$$

where $\alpha \approx 0.40$ and $\beta \approx 1/8$. The goodness of fit by equation (15) can be assessed by quantifying the fluctuation of the data points with respect to the straight line plotted in the logarithmic scales, as shown in Figure 4. To this end, the relative fluctuation for each data point was computed as $|\log(f_s^{\text{measured}}) - \log(f_s^{\text{predicted}})| / \log(f_s^{\text{predicted}})$. Statistics of the computed results show that on average, the relative fluctuation is 27.6%, which implies that equation (15) generally represents most of the data points.

[26] Substituting equations (8) and (14) into equation (15) and manipulating, we get the average flow velocity in the surface layer,

$$U_s = \eta \left(\frac{1 - \lambda h_s}{\lambda d} \right)^{1/16} \sqrt{g h_s S}, \quad (16)$$

where $\eta \approx 4.54$.

4.2. Calculation of Average Velocity and Resistance Coefficients

[27] As previously done by [Huthoff et al., 2007; Yang and Choi, 2010], the average velocity of the flow through the entire cross section can be computed by considering the surface and vegetation layers individually (see Figure 1). Using U_v to denote the average velocity of flow among vegetation stems, the average velocity through the entire cross section can be expressed as

$$U = \frac{U_s h_s + U_v h_v (1 - \lambda)}{H}. \quad (17)$$

As reported by Stone and Shen [2002] and also confirmed in the present study, the average velocity through the vegetation layer is very close to that observed for the case of emergent vegetation for the same energy slope and vegetation configuration. Therefore, U_v can be estimated using the drag coefficient C_D proposed earlier by Cheng and Nguyen [2011] for the emergent case,

$$U_v = \sqrt{\frac{2gr_v S}{C_D}}, \quad (18)$$

where

$$C_D = \frac{130}{r_{v*}^{0.85}} + 0.8 \left[1 - \exp\left(-\frac{r_{v*}}{400}\right) \right], \quad (19)$$

with $r_{v*} = (gS/\nu^2)^{1/3} r_v$, $r_v = \pi(1 - \lambda)d/(4\lambda)$ and ν is the kinematic viscosity of fluid. Considering that average

vegetation-layer velocities are usually not available for most of the datasets reported in the previous studies, equation (18) is applied to all the data for estimating U_v in the subsequent analyses.

[28] Substituting equations (16) and (18) into equation (17), we get,

$$U = \left[\sqrt{\frac{\pi(1-\lambda)^3 d}{2C_D \lambda}} \frac{h_v}{H} \right]^{3/2} + 4.54 \left(\frac{h_s(1-\lambda)}{d \lambda} \right)^{1/16} \left(\frac{h_s}{H} \right)^{3/2} \sqrt{gHS}. \quad (20)$$

Using equation (20), the chezy coefficient, i.e., $C = U/(HS)^{0.5}$, is expressed as,

$$C = \sqrt{\frac{\pi g}{2C_D} \frac{(1-\lambda)^3 d}{\lambda} \frac{h_v}{H}}^{3/2} + 4.54 \sqrt{g} \left(\frac{h_s(1-\lambda)}{d \lambda} \right)^{1/16} \left(\frac{h_s}{H} \right)^{3/2}. \quad (21)$$

Similarly, the expression for the Manning coefficient can also be obtained by noting that $n = H^{1/6}/C$.

4.3. Comparisons With Previous Formulas

[29] First, the values of the roughness height computed using the proposed formula, i.e., equation (8), are compared with other two formulas, i.e., equation (4) [Huthoff et al., 2007] and equation (6) [Baptist et al., 2007]. Figure 5 shows that equation (8) is comparable only to equation (4) with C_D computed using equation (19). In comparison, the results of y_o computed using equations (6) appear completely unrelated to k_v given by equation (8). This is understandable by noting that both equations (4) and (8) are proportional to the product of λd . However, it should be also mentioned that in Huthoff's study, the selection of stem spacing as characteristic length scale for the surface layer is somewhat arbitrary. In comparison, the framework presented in this study for defining the roughness length has a better physical basis.

[30] Second, the average velocities predicted using equation (20) are compared with four previous formulas as follows:

[31] 1. Stone and Shen's [2002] formula,

$$U = 1.385 \left(\frac{H}{h_v} \sqrt{\frac{\pi}{4\lambda}} - 1 \right) \sqrt{gdS}, \quad (22)$$

where S is the vegetation-related energy slope and close to the total energy slope if the bed friction is negligible.

[32] 2. Baptist et al.'s [2007] formula. By applying genetic programming (GP), a machine learning technique that performs optimization with symbolic operations, Baptist et al. obtained

$$U = \left[\sqrt{\frac{1}{g/C_b^2 + 2C_D \lambda h_v / (\pi d)}} + 2.5 \ln\left(\frac{H}{h_v}\right) \right] \sqrt{gHS}, \quad (23)$$

where C_b is the bed-related Chezy coefficient ($\approx 60 \text{ m}^{0.5} \text{ s}^{-1}$ for smooth bed), and C_D could be taken to be 1.0.

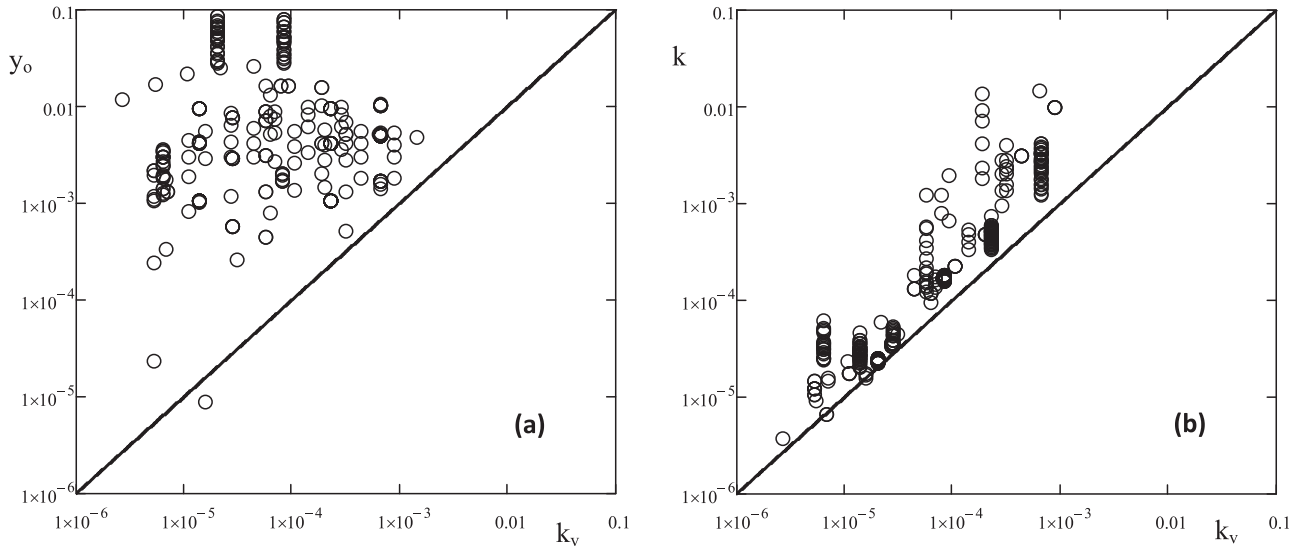


Figure 5. Comparisons of estimated roughness heights. They are computed using *Baptist et al.*'s [2007] formula (y_o given by equation (6)), *Huthoff et al.*'s [2007] formula (k by equation (4)) and the present formula (k_v by equation (8)). The unit is m.

[33] 3. *Huthoff et al.*'s [2007] formula. With similarity considerations, Huthoff et al. developed a scaling model for the entire flow depth, which yields the average velocity given by

$$U = \left[\frac{h_s}{H} \left(\frac{h_s}{(\sqrt{\pi}/(4\lambda) - 1)d} \right)^{\frac{2}{3} \left[1 - \left(\frac{h_s}{H} \right)^5 \right]} + \sqrt{\frac{h_v}{H}} \right] \sqrt{\frac{\pi g d S}{2 C_D \lambda}} \quad (24)$$

Huthoff et al. calibrated their model using the data by *Meijer and van Velzen* [1999], and also mentioned that C_D remains almost constant with a value of nearly 1.0.

[34] 4. *Yang and Choi*'s [2010] formula. By applying the logarithmic law to the surface layer, Yang and Choi recently proposed the depth-averaged velocity computed as

$$U = \sqrt{\frac{\pi g d H S}{2 C_D h_v \lambda}} + \frac{C_u \sqrt{g h_s S}}{0.41} \left(\ln \frac{H}{h_v} - \frac{h_s}{H} \right), \quad (25)$$

where $C_D = 1.13$, and $C_u = 1$ for $4\lambda/(\pi d) \leq 5$ and 2 for $4\lambda/(\pi d) > 5$.

[35] Table 3 summarized the average errors of predictions associated with equations (20) and (22)–(25). Here, the error

was computed as $|\text{prediction} - \text{measurement}|/\text{measurement}$. Altogether, 300 datasets were used, of which 23 were collected in the present study and the rest by the others. For each formula applied, the prediction error varies with the parameter predicted. On average, it can be observed that (1) the formulas proposed previously by *Baptist* [2007], *Stone and Shen* [2002], and *Yang and Choi* [2010] appear to be less accurate, and (2) although the formula proposed in this study performs almost the best, its accuracy is close to that of the formula by *Huthoff et al.* [2007].

[36] To show the comparisons in detail, the predictions by individual formula are plotted against the measurements in Figure 6. Here, we choose the flowrate as the variable for comparison by noting that the flowrate measured varies in a range much wider than other variables including average flow velocity, and Manning and Chezy coefficients. With the wide variation, the prediction errors can be displayed clearly, which makes possible to observe which formula performs well in what range of flow conditions. Figures 6a and 6d show that both Stone and Shen's and *Yang and Choi*'s [2010] formulas generally underestimate the flow rates. In particular, all high flow rates by *Meijer and van Velzen* [1999] were underestimated by these two formulas with the error of 34.0% and 41.9%, respectively.

Table 3. Prediction Errors for Different Formulas

Investigator	Equation	Absolute Error (%)			
		Rigid Vegetation		Flexible Vegetation	
		Flow Rate or Average Velocity or Chezy Coefficient	Manning Coefficient	Flow Rate or Average Velocity or Chezy Coefficient	Manning Coefficient
<i>Stone and Shen</i> [2002]	(22)	18.9	26.1	27.0	60.0
<i>Baptist et al.</i> [2007]	(23)	24.2	18.6	27.1	20.6
<i>Huthoff et al.</i> [2007]	(24)	14.0	18.0	15.3	18.7
<i>Yang and Choi</i> [2010]	(25)	20.9	30.8	15.7	21.9
Present study	(20)	14.3	16.8	16.6	15.2

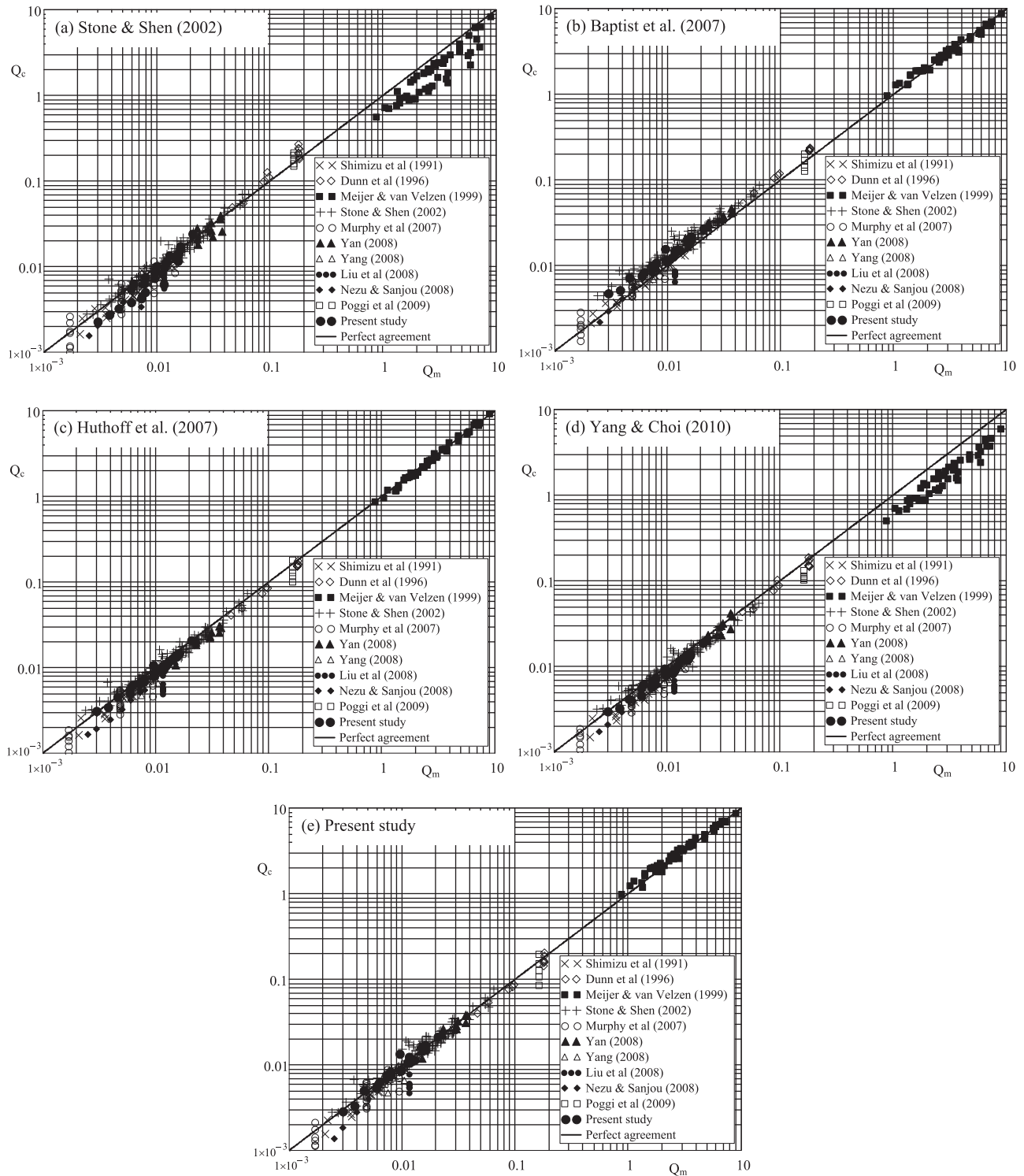


Figure 6. Comparisons of calculated flow rates (Q_c) with measurements (Q_m) (in $\text{m}^3 \text{s}^{-1}$) for the case of submerged rigid vegetation.

Baptist et al.'s [2007] formula works well for high flow rates, but yields overprediction for low flow rates (with the error of 27.3%) (see Figure 6b). *Huthoff et al.*'s [2007] formula gives the best prediction for high flow rates, but underestimates low flow rates (with the error of 15.8%), as shown in Figure 6c. This may be explained by the fact that

their model was calibrated solely with the high flowrate data by *Meijer and van Velzen* [1999], who conducted experiments in a large-scale flume (see Table 2).

[37] In comparison, being calibrated with the larger database, the formula proposed in this study applies equally well for both high and low flow rates (see Figure 6e), of which

Table 4. Values of the Five Constants Included in Equation (28)

Investigator	Equation	c_1	c_2	c_3	c_4	c_5
Stone and Shen [2002]	(22)	-1	-1.1	0.5	0	0
Baptist et al. [2007]	(23)	-0.5	4	0.5	0.5	1.5
Huthoff et al. [2007]	(24)	0.5	1.1	0.33	0.67	1.67
Yang and Choi [2010]	(25)	-0.5	1.1-2.2	0.5	0.5	2.5
Present study	(20)	1	5.1	0.5	0.5	1.5

the prediction errors are 15.3% and 9.0%, respectively. However, it should be mentioned that the good agreement is not surprising by noting that the data for comparison are the same as those used for developing equation (15).

5. Discussion

5.1. Simplification of Formulas

[38] It is noted that the five formulas compared in section 4 appear in the different forms because they have been derived with different considerations. However, for some simple conditions, they can also be reduced and expressed similarly. Such an attempt is given as follows.

[39] First, consider the case of emergent vegetation, for which $h_s = 0$ and $H = h_v$. Then, equation (20) reduces to

$$U_v = 1.25 \sqrt{\frac{(1 - \lambda)^3 dgS}{C_D \lambda}} \tag{26}$$

Furthermore, if assuming that $\lambda \ll 1$ and $C_D \approx 1$, equation (26) can be rewritten as

$$U_v = 1.25 \sqrt{\frac{dgS}{\lambda}} \tag{27}$$

It can be shown that equation (27) can also be obtained by simplifying equations (22) to (24) for the same condition.

[40] Next, with the assumptions of $\lambda \ll 1$ and $C_D \approx 1$ and equation (27), we can rewrite all velocity formulas, i.e., equations (20) and (22)–(25), in the following general form,

$$\frac{U}{U_v} = \left(\frac{h_v}{H}\right)^{c_1} + c_2 \lambda^{c_3} \left(\frac{H}{d}\right)^{c_4} \left(1 - \frac{h_v}{H}\right)^{c_5} \tag{28}$$

where constants c_1 to c_5 are given in Table 4 for each formula. To simplify equation (20), we note that $[(h_s/d)(1 - \lambda)/\lambda]^{1/16}$ varies in a limited range, and could be replaced with a constant of 1.6 that was estimated using the data collected. In addition, we also replace $\ln(H/h_v)$ in equation (23) using $2(1 - h_v/H)^{1.5}$ with an accuracy of 4.8% for $H/h_v = 1.5 - 4$. Similarly, to rewrite equation (25), we use $0.56(1 - h_v/H)^{2.5}$ to approximate $[\ln(H/h_v) - (1 - h_v/H)][h_v/H(1 - h_v/H)]^{0.5}$ with an accuracy of 3.8% for $H/h_v = 1.5 - 4$. From the constants summarized in Table 4, it follows that although derived from the different considerations, the five formulas except for equation (22) appear similar by noting that each of constants c_3 to c_5 has close values for the different formulas.

[41] With equation (28) together with each set of constants given in Table 4, we also performed additional computations using the data summarized in Table 2. The results indicate that the predictions made using the simplified formula differ to some extent from those using the complete version (see Table 5). For the formulas proposed by Stone and Shen [2002] and Baptist et al. [2007], it is surprising to note that the simplified versions even provide improved predictions, with prediction errors reduced by 0.1–1.3%. In comparison, the other three formulas including the present formula, if applied in the simplified version, all lead to worse predictions, and the corresponding errors increase by 1.4–5.7%. Due to the replacement with a universal constant (1.6), the simplification of the formula proposed in this study causes the largest error difference of 4.0–5.7%.

5.2. Application to Submerged Flexible Vegetation

[42] Complex fluid dynamics are involved in interactions between flexible vegetation and flow, which are not investigated in this study. In the following, we will check, to what extent, equation (20) can be used to predict the average flow velocity in the presence of submerged flexible vegetation. Altogether 103 sets of data are used here, which were reported previously by Dunn et al. [1996], Jarvela [2003], Kouwen et al. [1969], Kubrak et al. [2008], Okamoto and Nezu [2010], and Yang [2008]. It is noted that different materials have been employed to simulate flexible vegetation, including film strips [Kouwen et al., 1969; Okamoto and Nezu, 2010; Yang, 2008], cylindrical stems [Dunn et al., 1996; Kubrak et al., 2008] and real plants [Jarvela, 2003]. In applying equation (20), h_v is taken as the average value of deflected height, which partially reflects the effect

Table 5. Error Differences of Predictions With Formulas in Complete and Simplified Versions^a

Investigator	Difference of Absolute Errors (%)			
	Rigid Vegetation		Flexible Vegetation	
	Flow Rate or Average Velocity or Chezy Coefficient	Manning Coefficient	Flow Rate or Average Velocity or Chezy Coefficient	Manning Coefficient
Stone and Shen [2002]	-0.3	-1.3	-0.3	-2.4
Baptist et al. [2007]	-0.5	-0.1	-2.0	-1.2
Huthoff et al. [2007]	1.4	2.6	6.8	10.1
Yang and Choi [2010]	1.4	2.7	11.6	28.2
Present study	4.0	5.7	2.3	3.2

^aThe error difference was computed as absolute error (%) of prediction using a formula in the complete version – absolute error (%) of prediction using the formula in the simplified version.

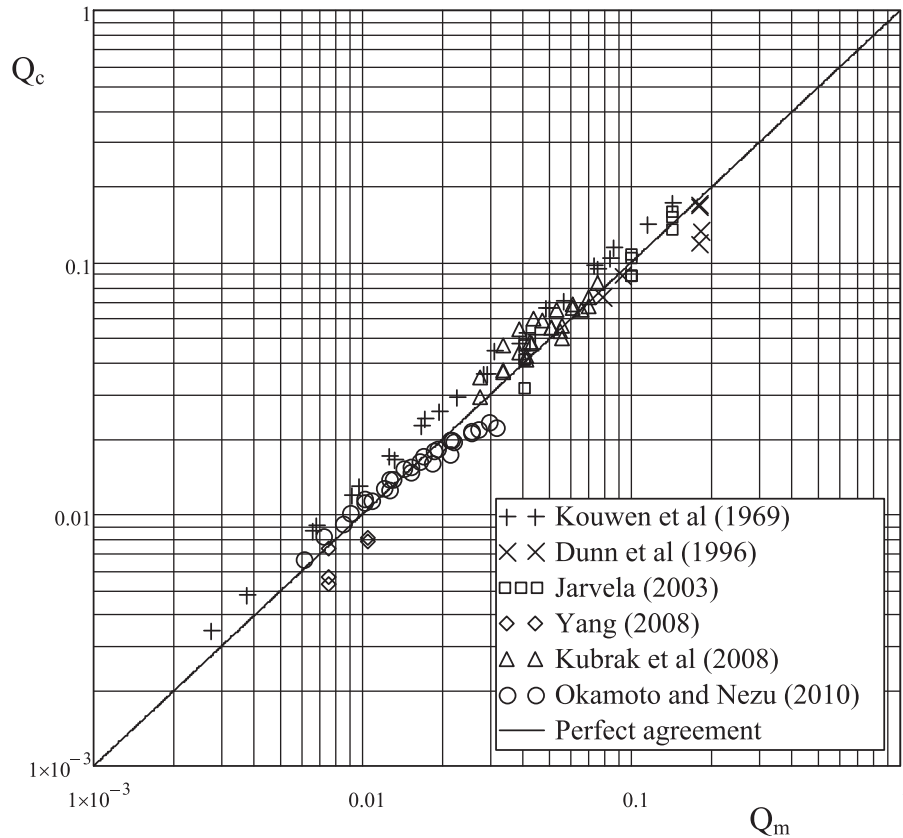


Figure 7. Comparison of calculated flow rates (Q_c) with measurements (Q_m) (in $\text{m}^3 \text{s}^{-1}$) for the case of submerged flexible vegetation.

of flexibility. For film strips, as mentioned in section 3.3.4, the equivalent concentration λ is computed as $\pi Nd^2/4$, where d is the strip width, and N is the number of strips per unit area. The computed flow rates are plotted against the data in Figure 7, showing that the agreement is generally acceptable. The average of absolute errors of the prediction is 16.6%.

[43] When applying *Stone and Shen's* [2002] and *Baptist et al.'s* [2007] formulas in their simplified versions, the predictions are slightly improved as for the case of rigid vegetation. The absolute error reduces by 0.3 to 2.4% (see Table 5). In comparison, for the other three formulas, the simplified versions yield worse predictions. The prediction error increases by 11.6–28.2% for *Yang and Choi's* [2010] formula, and 6.8–10.1% for *Huthoff et al.'s* [2007] formula. The increase in the error for the formula proposed in this study is relatively small, i.e., from 2.3% to 3.2%.

6. Summary

[44] By considering the relative blockage caused by submerged vegetation, a representative roughness height is proposed for the description of resistance of vegetated open channel flows. This roughness height is characterized by its proportionality to both stem diameter and vegetation density. The analysis shows that the friction factor defined for the surface layer above the vegetation slightly increases with increasing relative roughness height, the latter being taken as the ratio of the roughness height to the surface

layer thickness. The resistance relationship can be approximated using a power law function, which yields improved predictions in particular for the case of low flow rates, in comparison with the previous formulas. In addition, it is also shown that all formulas, when simplified for some simple conditions, can be expressed in a general form, although they have been derived with different arguments.

[45] Although most of the data used for the analyses in this study were collected for vegetation simulated with rigid, cylindrical rods, the application of the proposed formula for the case of flexible vegetation also shows acceptable results. However, it should be mentioned that effects of vegetation flexibility on the flow resistance have not been fully incorporated in the analysis.

Appendix A

[46] Several experimental works that are similar to the present study have been conducted previously to investigate open channel flows subject to submerged rigid or flexible vegetation. From these studies, 277 sets of data were gathered for the case of rigid vegetation and 103 sets of data for the case of flexible vegetation. All these data are listed in Table A1, in terms of eight variables, i.e., channel width (B), flow depth (H), energy slope (S), discharge (Q), stem diameter or strip width (d), vegetation height (h_v), concentration (λ) and number of stems or strips per unit area (N).

Table A1. Compilation of Experimental Data of Open Channel Flows With Submerged Vegetation

	No.	Run	Q (m ³ s ⁻¹)	B (m)	H (m)	S	λ	d (m)	h_v (m)	N (m ⁻²)	
	<i>(A) Rigid Vegetation</i>										
<i>Shimizu et al. [1991]</i>	R1	R21	0.002,073	0.5	0.0636	0.00,066	0.00,785	0.001	0.041	9995	
	R2	R22	0.003,486	0.5	0.073	0.00,108	0.00,785	0.001	0.041	9995	
	R3	R23	0.004,786	0.5	0.0883	0.0009	0.00,785	0.001	0.041	9995	
	R4	R24	0.006,058	0.5	0.0948	0.001	0.00,785	0.001	0.041	9995	
	R5	R25	0.007,736	0.5	0.1054	0.00,099	0.00,785	0.001	0.041	9995	
	R6	R31	0.003,537	0.5	0.0631	0.00,164	0.00,785	0.001	0.041	9995	
	R7	R32	0.00,518	0.5	0.0747	0.00,213	0.00,785	0.001	0.041	9995	
	R8	R33	0.006,841	0.5	0.0842	0.00,201	0.00,785	0.001	0.041	9995	
	R9	R34	0.008,558	0.5	0.0941	0.00,183	0.00,785	0.001	0.041	9995	
	R10	R35	0.010,552	0.5	0.1061	0.00,176	0.00,785	0.001	0.041	9995	
	R11	R41	0.004,784	0.5	0.0659	0.00,233	0.00,785	0.001	0.041	9995	
	R12	R42	0.006,306	0.5	0.0735	0.00,263	0.00,785	0.001	0.041	9995	
	R13	R43	0.008,508	0.5	0.0847	0.00,304	0.00,785	0.001	0.041	9995	
	R14	R44	0.010,512	0.5	0.0953	0.00,256	0.00,785	0.001	0.041	9995	
	R15	R45	0.014,154	0.5	0.1026	0.0032	0.00,785	0.001	0.041	9995	
	R16	R51	0.006,129	0.5	0.0659	0.00,455	0.00,785	0.001	0.041	9995	
	R17	R52	0.007,541	0.5	0.0739	0.00,455	0.00,785	0.001	0.041	9995	
	R18	R53	0.009,802	0.5	0.0841	0.00,435	0.00,785	0.001	0.041	9995	
	R19	R54	0.012,944	0.5	0.0956	0.00,435	0.00,785	0.001	0.041	9995	
	R20	R55	0.016,022	0.5	0.1052	0.00,476	0.00,785	0.001	0.041	9995	
	R21	A11	0.005,035	0.4	0.095	0.001	0.00,442	0.0015	0.046	2501	
	R22	A12	0.003,511	0.4	0.0749	0.001	0.00,442	0.0015	0.046	2501	
	R23	A31	0.007,334	0.4	0.0936	0.003	0.00,442	0.0015	0.046	2501	
	R24	A32	0.005,274	0.4	0.0735	0.003	0.00,442	0.0015	0.046	2501	
	R25	A34	0.00,216	0.4	0.05	0.003	0.00,442	0.0015	0.046	2501	
	R26	A35	0.002,806	0.4	0.0568	0.003	0.00,442	0.0015	0.046	2501	
	R27	A71	0.011,832	0.4	0.0895	0.007	0.00,442	0.0015	0.046	2501	
	R28	A72	0.007,761	0.4	0.0727	0.007	0.00,442	0.0015	0.046	2501	
<i>Dunn et al. [1996]</i>	R29	1	0.179	0.91	0.335	0.0036	0.005,436	0.00,635	0.1175	172	
	R30	2	0.088	0.91	0.229	0.0036	0.005,436	0.00,635	0.1175	172	
	R31	3	0.046	0.91	0.164	0.0036	0.005,436	0.00,635	0.1175	172	
	R32	4	0.178	0.91	0.276	0.0076	0.005,436	0.00,635	0.1175	172	
	R33	5	0.098	0.91	0.203	0.0076	0.005,436	0.00,635	0.1175	172	
	R34	6	0.178	0.91	0.267	0.0036	0.001,362	0.00,635	0.1175	43	
	R35	7	0.095	0.91	0.183	0.0036	0.001,362	0.00,635	0.1175	43	
	R36	8	0.18	0.91	0.391	0.0036	0.012,269	0.00,635	0.1175	387	
	R37	9	0.058	0.91	0.214	0.0036	0.012,269	0.00,635	0.1175	387	
	R38	10	0.18	0.91	0.265	0.0161	0.012,269	0.00,635	0.1175	387	
	R39	11	0.177	0.91	0.311	0.0036	0.003,067	0.00,635	0.1175	97	
	R40	12	0.181	0.91	0.233	0.0108	0.003,067	0.00,635	0.1175	97	
<i>Meijer [1998]</i> <i>[see Baptist, 2005]</i>	R41	1	1.0395	3	1.98	0.00,109	0.012,868	0.008	1.5	256	
	R42	2	1.39,101	3	1.99	0.0018	0.012,868	0.008	1.5	256	
	R43	3	1.39,284	3	2.19	0.00,095	0.012,868	0.008	1.5	256	
	R44	4	1.56,366	3	2.19	0.00,125	0.012,868	0.008	1.5	256	
	R45	5	1.7061	3	2.35	0.00,081	0.012,868	0.008	1.5	256	
	R46	6	2.35,563	3	2.33	0.00,154	0.012,868	0.008	1.5	256	
	R47	7	1.9125	3	2.5	0.00,065	0.012,868	0.008	1.5	256	
	R48	8	2.72,688	3	2.47	0.00,143	0.012,868	0.008	1.5	256	
	R49	9	1.86,327	3	2.01	0.00,106	0.003,217	0.008	1.5	64	
	R50	10	2.52,657	3	2.01	0.00,193	0.003,217	0.008	1.5	64	
	R51	11	2.2902	3	2.2	0.00,101	0.003,217	0.008	1.5	64	
	R52	12	3.07,476	3	2.19	0.00,188	0.003,217	0.008	1.5	64	
	R53	13	2.6226	3	2.35	0.00,093	0.003,217	0.008	1.5	64	
	R54	14	3.45,807	3	2.31	0.00,187	0.003,217	0.008	1.5	64	
	R55	15	2.90,904	3	2.48	0.00,094	0.003,217	0.008	1.5	64	
	R56	16	3.9483	3	2.46	0.00,178	0.003,217	0.008	1.5	64	
	R57	17	1.12,344	3	1.51	0.00,107	0.012,868	0.008	0.9	256	
	R58	18	1.6188	3	1.52	0.00,204	0.012,868	0.008	0.9	256	
	R59	19	1.79,733	3	1.81	0.00,085	0.012,868	0.008	0.9	256	
	R60	20	2.5542	3	1.8	0.00,165	0.012,868	0.008	0.9	256	
	R61	21	2.52,681	3	2.09	0.00,071	0.012,868	0.008	0.9	256	
	R62	22	3.61,779	3	2.09	0.00,138	0.012,868	0.008	0.9	256	
	R63	23	3.72	3	2.48	0.00,055	0.012,868	0.008	0.9	256	
	R64	24	5.96,304	3	2.46	0.00,149	0.012,868	0.008	0.9	256	
	R65	25	1.74,858	3	1.51	0.00,103	0.003,217	0.008	0.9	64	
	R66	26	2.52,624	3	1.52	0.00,205	0.003,217	0.008	0.9	64	
	R67	27	2.50,323	3	1.81	0.00,085	0.003,217	0.008	0.9	64	
	R68	28	3.52,974	3	1.78	0.0018	0.003,217	0.008	0.9	64	
	R69	29	3.3831	3	2.1	0.00,075	0.003,217	0.008	0.9	64	

Table A1. (continued)

	No.	Run	Q ($\text{m}^3 \text{s}^{-1}$)	B (m)	H (m)	S	λ	d (m)	h_v (m)	N (m^{-2})
	R70	30	4.72,152	3	2.06	0.00,164	0.003,217	0.008	0.9	64
	R71	31	4.77,945	3	2.47	0.00,071	0.003,217	0.008	0.9	64
	R72	32	6.68,382	3	2.47	0.00,143	0.003,217	0.008	0.9	64
	R73	33	0.86,598	3	1.02	0.00,078	0.012,868	0.008	0.45	256
	R74	34	1.30,977	3	0.99	0.00,164	0.012,868	0.008	0.45	256
	R75	35	2.08,833	3	1.51	0.00,059	0.012,868	0.008	0.45	256
	R76	36	3.06	3	1.5	0.00,138	0.012,868	0.008	0.45	256
	R77	37	3.7422	3	1.98	0.00,058	0.012,868	0.008	0.45	256
	R78	38	5.62,374	3	1.99	0.00,142	0.012,868	0.008	0.45	256
	R79	39	5.91,876	3	2.46	0.0007	0.012,868	0.008	0.45	256
	R80	40	7.17,867	3	2.49	0.0009	0.012,868	0.008	0.45	256
	R81	41	1.34,028	3	1.02	0.00,075	0.003,217	0.008	0.45	64
	R82	42	1.983	3	1	0.00,187	0.003,217	0.008	0.45	64
	R83	43	2.808	3	1.5	0.00,069	0.003,217	0.008	0.45	64
	R84	44	4.7745	3	1.5	0.00,199	0.003,217	0.008	0.45	64
	R85	45	5.73	3	2	0.00,099	0.003,217	0.008	0.45	64
	R86	46	7.314	3	2	0.00,159	0.003,217	0.008	0.45	64
	R87	47	6.56,952	3	2.48	0.00,063	0.003,217	0.008	0.45	64
	R88	48	8.97,966	3	2.41	0.00,127	0.003,217	0.008	0.45	64
Stone and Shen [2002] [see Stone, 1997]	R89	S9	5.70E-03	0.45	0.151	2.32E-03	0.061	0.013	0.124	460
	R90	S22	3.20E-03	0.45	0.155	9.10E-04	0.061	0.013	0.124	460
	R91	S23	4.80E-03	0.45	0.155	1.59E-03	0.061	0.013	0.124	460
	R92	S24	8.20E-03	0.45	0.155	4.06E-03	0.061	0.013	0.124	460
	R93	S25	0.011	0.45	0.155	7.61E-03	0.061	0.013	0.124	460
	R94	S26	0.017	0.45	0.155	0.017	0.061	0.013	0.124	460
	R95	S27	0.026	0.45	0.155	0.032	0.061	0.013	0.124	460
	R96	S28	2.40E-03	0.45	0.155	5.50E-04	0.061	0.013	0.124	460
	R97	S51	2.70E-03	0.45	0.153	5.90E-04	0.061	0.013	0.124	460
	R98	S52	4.30E-03	0.45	0.155	1.44E-03	0.061	0.013	0.124	460
	R99	S53	7.10E-03	0.45	0.155	3.34E-03	0.061	0.013	0.124	460
	R100	S54	0.029	0.45	0.155	0.044	0.061	0.013	0.124	460
	R101	S29	4.50E-03	0.45	0.206	4.50E-04	0.061	0.013	0.124	460
	R102	S30	6.00E-03	0.45	0.207	6.30E-04	0.061	0.013	0.124	460
	R103	S31	8.70E-03	0.45	0.205	9.40E-04	0.061	0.013	0.124	460
	R104	S32	0.012	0.45	0.205	1.98E-03	0.061	0.013	0.124	460
	R105	S33	0.018	0.45	0.206	4.45E-03	0.061	0.013	0.124	460
	R106	S34	0.029	0.45	0.207	0.012	0.061	0.013	0.124	460
	R107	S35	0.023	0.45	0.207	7.42E-03	0.061	0.013	0.124	460
	R108	S36	6.90E-03	0.45	0.207	8.10E-04	0.061	0.013	0.124	460
R109	S46	5.00E-03	0.45	0.206	5.90E-04	0.061	0.013	0.124	460	
R110	S47	6.60E-03	0.45	0.209	5.40E-04	0.061	0.013	0.124	460	
R111	S48	8.00E-03	0.45	0.206	9.00E-04	0.061	0.013	0.124	460	
R112	S49	9.20E-03	0.45	0.207	1.17E-03	0.061	0.013	0.124	460	
R113	S50	0.011	0.45	0.212	1.34E-03	0.061	0.013	0.124	460	
R114	S37	0.01	0.45	0.311	3.60E-04	0.061	0.013	0.124	460	
R115	S38	0.011	0.45	0.308	5.40E-04	0.061	0.013	0.124	460	
R116	S39	0.016	0.45	0.308	7.60E-04	0.061	0.013	0.124	460	
R117	S40	0.021	0.45	0.311	9.30E-04	0.061	0.013	0.124	460	
R118	S41	0.013	0.45	0.314	4.00E-04	0.061	0.013	0.124	460	
R119	S42	0.028	0.45	0.308	1.88E-03	0.061	0.013	0.124	460	
R120	S43	0.013	0.45	0.308	3.50E-04	0.061	0.013	0.124	460	
R121	S44	0.011	0.45	0.308	4.70E-04	0.061	0.013	0.124	460	
R122	S45	0.015	0.45	0.311	5.40E-04	0.061	0.013	0.124	460	
R123	S66	3.80E-03	0.45	0.155	3.50E-04	0.022	0.013	0.124	166	
R124	S67	4.90E-03	0.45	0.155	5.80E-04	0.022	0.013	0.124	166	
R125	S68	7.10E-03	0.45	0.155	1.03E-03	0.022	0.013	0.124	166	
R126	S69	8.90E-03	0.45	0.155	1.70E-03	0.022	0.013	0.124	166	
R127	S70	0.011	0.45	0.155	2.75E-03	0.022	0.013	0.124	166	
R128	S71	0.017	0.45	0.155	5.23E-03	0.022	0.013	0.124	166	
R129	S72	0.028	0.45	0.155	0.014	0.022	0.013	0.124	166	
R130	S90	0.018	0.45	0.155	5.68E-03	0.022	0.013	0.124	166	
R131	S91	0.021	0.45	0.155	8.38E-03	0.022	0.013	0.124	166	
R132	S94	0.023	0.45	0.155	0.01	0.022	0.013	0.124	166	
R133	S95	0.015	0.45	0.155	4.52E-03	0.022	0.013	0.124	166	
R134	S99	6.60E-03	0.45	0.155	9.80E-04	0.022	0.013	0.124	166	
R135	S109	8.90E-03	0.45	0.155	2.07E-03	0.022	0.013	0.124	166	
R136	S110	7.10E-03	0.45	0.155	1.18E-03	0.022	0.013	0.124	166	
R137	S119	0.013	0.45	0.155	3.14E-03	0.022	0.013	0.124	166	
R138	S120	0.019	0.45	0.155	6.79E-03	0.022	0.013	0.124	166	

Table A1. (continued)

No.	Run	Q ($\text{m}^3 \text{s}^{-1}$)	B (m)	H (m)	S	λ	d (m)	h_v (m)	N (m^{-2})
R139	S121	0.023	0.45	0.155	9.52E-03	0.022	0.013	0.124	166
R140	S73	4.60E-03	0.45	0.207	2.30E-04	0.022	0.013	0.124	166
R141	S74	5.90E-03	0.45	0.207	2.70E-04	0.022	0.013	0.124	166
R142	S75	6.90E-03	0.45	0.207	3.60E-04	0.022	0.013	0.124	166
R143	S76	8.10E-03	0.45	0.207	6.30E-04	0.022	0.013	0.124	166
R144	S77	9.40E-03	0.45	0.207	5.30E-04	0.022	0.013	0.124	166
R145	S78	0.011	0.45	0.207	7.10E-04	0.022	0.013	0.124	166
R146	S79	0.017	0.45	0.207	1.53E-03	0.022	0.013	0.124	166
R147	SS0	0.029	0.45	0.207	4.28E-03	0.022	0.013	0.124	166
R148	S92	0.025	0.45	0.207	3.82E-03	0.022	0.013	0.124	166
R149	S93	0.021	0.45	0.207	2.34E-03	0.022	0.013	0.124	166
R150	S97	6.80E-03	0.45	0.207	3.50E-04	0.022	0.013	0.124	166
R151	S98	0.015	0.45	0.207	1.23E-03	0.022	0.013	0.124	166
R152	S108	7.70E-03	0.45	0.207	5.40E-04	0.022	0.013	0.124	166
R153	S126	0.013	0.45	0.207	8.90E-04	0.022	0.013	0.124	166
R154	S127	0.019	0.45	0.207	1.95E-03	0.022	0.013	0.124	166
R155	S128	0.024	0.45	0.207	3.63E-03	0.022	0.013	0.124	166
R156	S81	0.011	0.45	0.308	4.50E-04	0.022	0.013	0.124	166
R157	S82	9.50E-03	0.45	0.308	9.00E-05	0.022	0.013	0.124	166
R158	S83	0.013	0.45	0.308	3.60E-04	0.022	0.013	0.124	166
R159	S84	0.015	0.45	0.308	4.50E-04	0.022	0.013	0.124	166
R160	S85	0.017	0.45	0.308	5.40E-04	0.022	0.013	0.124	166
R161	S86	0.027	0.45	0.308	7.90E-04	0.022	0.013	0.124	166
R162	S101	0.029	0.45	0.308	1.47E-03	0.022	0.013	0.124	166
R163	S122	0.012	0.45	0.308	2.20E-04	0.022	0.013	0.124	166
R164	S123	0.019	0.45	0.308	4.00E-04	0.022	0.013	0.124	166
R165	S124	0.024	0.45	0.308	6.60E-04	0.022	0.013	0.124	166
R166	S146	6.60E-03	0.45	0.155	9.80E-04	5.50E-03	3.18E-03	0.124	692
R167	S147	7.60E-03	0.45	0.155	1.16E-03	5.50E-03	3.18E-03	0.124	692
R168	S148	0.01	0.45	0.155	1.87E-03	5.50E-03	3.18E-03	0.124	692
R169	S149	0.014	0.45	0.155	4.57E-03	5.50E-03	3.18E-03	0.124	692
R170	S150	0.019	0.45	0.155	4.43E-03	5.50E-03	3.18E-03	0.124	692
R171	S151	0.028	0.45	0.155	0.011	5.50E-03	3.18E-03	0.124	692
R172	S153	5.50E-03	0.45	0.155	5.40E-04	5.50E-03	3.18E-03	0.124	692
R173	S154	0.011	0.45	0.155	2.05E-03	5.50E-03	3.18E-03	0.124	692
R174	S155	3.90E-03	0.45	0.154	2.60E-04	5.50E-03	3.18E-03	0.124	692
R175	S156	0.022	0.45	0.155	6.76E-03	5.50E-03	3.18E-03	0.124	692
R176	RS146	6.10E-03	0.45	0.155	7.60E-04	5.50E-03	3.18E-03	0.124	692
R177	RS147	7.50E-03	0.45	0.155	8.40E-04	5.50E-03	3.18E-03	0.124	692
R178	RS148	0.01	0.45	0.155	1.73E-03	5.50E-03	3.18E-03	0.124	692
R179	RS154	0.011	0.45	0.155	1.87E-03	5.50E-03	3.18E-03	0.124	692
R180	RS156	0.022	0.45	0.155	6.94E-03	5.50E-03	3.18E-03	0.124	692
R181	S157	3.70E-03	0.45	0.207	2.70E-04	5.50E-03	3.18E-03	0.124	692
R182	S158	6.70E-03	0.45	0.208	1.70E-04	5.50E-03	3.18E-03	0.124	692
R183	S159	0.011	0.45	0.209	5.30E-04	5.50E-03	3.18E-03	0.124	692
R184	S160	0.014	0.45	0.206	1.06E-03	5.50E-03	3.18E-03	0.124	692
R185	S161	0.028	0.45	0.206	3.72E-03	5.50E-03	3.18E-03	0.124	692
R186	S167	0.022	0.45	0.207	2.31E-03	5.50E-03	3.18E-03	0.124	692
R187	S168	0.024	0.45	0.206	2.73E-03	5.50E-03	3.18E-03	0.124	692
R188	S170	0.019	0.45	0.208	1.62E-03	5.50E-03	3.18E-03	0.124	692
R189	S171	8.90E-03	0.45	0.205	2.60E-04	5.50E-03	3.18E-03	0.124	692
R190	S172	0.027	0.45	0.205	3.65E-03	5.50E-03	3.18E-03	0.124	692
R191	S173	0.054	0.45	0.205	0.015	5.50E-03	3.18E-03	0.124	692
R192	S162	0.016	0.45	0.308	4.00E-04	5.50E-03	3.18E-03	0.124	692
R193	S163	0.022	0.45	0.308	5.70E-04	5.50E-03	3.18E-03	0.124	692
R194	S164	0.027	0.45	0.308	8.80E-04	5.50E-03	3.18E-03	0.124	692
R195	S165	0.042	0.45	0.308	2.03E-03	5.50E-03	3.18E-03	0.124	692
R196	S166	0.065	0.45	0.308	5.22E-03	5.50E-03	3.18E-03	0.124	692
R197	S169	0.024	0.45	0.311	5.30E-04	5.50E-03	3.18E-03	0.124	692
R198	S174	9.80E-03	0.45	0.308	9.00E-05	5.50E-03	3.18E-03	0.124	692
R199	S175	0.017	0.45	0.308	1.70E-04	5.50E-03	3.18E-03	0.124	692
R200	S176	0.027	0.45	0.308	8.80E-04	5.50E-03	3.18E-03	0.124	692
R201	S177	0.054	0.45	0.311	3.08E-03	5.50E-03	3.18E-03	0.124	692
R202	S207	0.011	0.45	0.155	1.08E-03	5.50E-03	6.35E-03	0.124	174
R203	S208	0.027	0.45	0.155	7.03E-03	5.50E-03	6.35E-03	0.124	174
R204	S209	0.02	0.45	0.155	4.13E-03	5.50E-03	6.35E-03	0.124	174
R205	S211	0.017	0.45	0.155	2.55E-03	5.50E-03	6.35E-03	0.124	174
R206	S212	9.50E-03	0.45	0.155	8.30E-04	5.50E-03	6.35E-03	0.124	174
R207	S210	8.70E-03	0.45	0.205	2.60E-04	5.50E-03	6.35E-03	0.124	174

Table A1. (continued)

	No.	Run	Q ($m^3 s^{-1}$)	B (m)	H (m)	S	λ	d (m)	h_v (m)	N (m^{-2})
	R208	S213	0.014	0.45	0.205	6.10E-04	5.50E-03	6.35E-03	0.124	174
	R209	S214	0.02	0.45	0.205	1.27E-03	5.50E-03	6.35E-03	0.124	174
	R210	S215	0.028	0.45	0.205	2.39E-03	5.50E-03	6.35E-03	0.124	174
	R211	S216	0.039	0.45	0.205	4.94E-03	5.50E-03	6.35E-03	0.124	174
	R212	S217	0.058	0.45	0.205	9.51E-03	5.50E-03	6.35E-03	0.124	174
	R213	S21S	0.021	0.45	0.31	3.40E-04	5.50E-03	6.35E-03	0.124	174
	R214	S219	0.028	0.45	0.31	4.50E-04	5.50E-03	6.35E-03	0.124	174
	R215	S220	0.04	0.45	0.31	1.17E-03	5.50E-03	6.35E-03	0.124	174
	R216	S221	0.057	0.45	0.31	2.57E-03	5.50E-03	6.35E-03	0.124	174
<i>Poggi et al. [2004]</i>	R217	D1	0.162	0.6	0.9	0.00,004	0.000,842	0.004	0.12	67
	R218	D2	0.162	0.6	0.9	0.00,007	0.001,684	0.004	0.12	134
	R219	D3	0.162	0.6	0.9	0.00,011	0.003,368	0.004	0.12	268
	R220	D4	0.162	0.6	0.9	0.00,018	0.006,736	0.004	0.12	536
	R221	D5	0.162	0.6	0.9	0.00,032	0.013,471	0.004	0.12	1072
<i>Murphy et al. [2007]</i>	R222	A	0.0048	0.38	0.467	9.9E-06	0.011,781	0.006	0.14	417
	R223	C	0.0074	0.38	0.467	0.000,025	0.016,022	0.006	0.14	567
	R224	D	0.0048	0.38	0.467	0.000,012	0.016,022	0.006	0.14	567
	R225	E	0.0143	0.38	0.467	0.000,075	0.01,885	0.006	0.14	667
	R226	G	0.0048	0.38	0.467	0.000,013	0.01,885	0.006	0.14	667
	R227	H	0.0143	0.38	0.467	0.0001	0.037,699	0.006	0.14	1333
	R228	I	0.0094	0.38	0.467	0.000,034	0.037,699	0.006	0.14	1333
	R229	A6	0.0017	0.38	0.298	0.000,003	0.011,781	0.006	0.07	417
	R230	B6	0.0094	0.38	0.298	8.04E-05	0.011,781	0.006	0.07	417
	R231	C6	0.0048	0.38	0.298	2.42E-05	0.011,781	0.006	0.07	417
	R232	A1	0.0017	0.38	0.236	1.06E-05	0.011,781	0.006	0.07	417
	R233	B1	0.0094	0.38	0.236	0.000,116	0.011,781	0.006	0.07	417
	R234	C1	0.0048	0.38	0.236	4.27E-05	0.011,781	0.006	0.07	417
	R235	A2	0.0017	0.38	0.14	1.73E-05	0.011,781	0.006	0.07	417
	R236	B2	0.0094	0.38	0.14	0.000,487	0.011,781	0.006	0.07	417
	R237	C2	0.0048	0.38	0.14	0.000,301	0.011,781	0.006	0.07	417
	R238	A3	0.0017	0.38	0.105	0.000,124	0.011,781	0.006	0.07	417
	R239	C3	0.0048	0.38	0.105	0.000,666	0.011,781	0.006	0.07	417
	R240	A5	0.0017	0.38	0.088	0.000,284	0.011,781	0.006	0.07	417
	R241	C5	0.0048	0.38	0.088	0.00,134	0.011,781	0.006	0.07	417
	R242	C6D	0.0048	0.38	0.298	2.03E-05	0.037,699	0.006	0.07	1333
	R243	C2D	0.0048	0.38	0.14	0.000,366	0.037,699	0.006	0.07	1333
	R244	A2D	0.0017	0.38	0.14	4.74E-05	0.037,699	0.006	0.07	1333
	R245	A3D	0.0017	0.38	0.105	0.000,232	0.037,699	0.006	0.07	1333
<i>Liu et al. [2008]</i>	R246	L1.4	0.0114	0.3	0.097	0.003	0.006,136	0.00,635	0.076	194
	R247	L1.5	0.0114	0.3	0.101	0.003	0.012,272	0.00,635	0.076	388
	R248	L1.6	0.0114	0.3	0.087	0.003	0.003,068	0.00,635	0.076	97
	R249	L3.1	0.0114	0.3	0.114	0.003	0.015,708	0.00,635	0.076	496
	R250	L3.2	0.0114	0.3	0.115	0.003	0.015,708	0.00,635	0.076	496
	R251	L3.3	0.0114	0.3	0.118	0.003	0.015,708	0.00,635	0.076	496
	R252	L3.4	0.0114	0.3	0.119	0.003	0.015,708	0.00,635	0.076	496
	R253	L3.5	0.0114	0.3	0.114	0.003	0.015,708	0.00,635	0.076	496
	R254	L3.6	0.0114	0.3	0.119	0.003	0.015,708	0.00,635	0.076	496
<i>Nezu and Sanjou [2008]</i>	R255	A-10	0.0072	0.4	0.15	0.000,777	0.1848	0.008	0.05	3676
	R256	B-10	0.0072	0.4	0.15	0.000,652	0.0924	0.008	0.05	1838
	R257	C-10	0.0072	0.4	0.15	0.000,544	0.0476	0.008	0.05	947
	R258	C-21	0.0025	0.4	0.0625	0.001,553	0.0476	0.008	0.05	947
	R259	C-22	0.003	0.4	0.075	0.001,165	0.0476	0.008	0.05	947
	R260	C-23	0.004	0.4	0.1	0.000,653	0.0476	0.008	0.05	947
	R261	C-24	0.005	0.4	0.125	0.00,046	0.0476	0.008	0.05	947
	R262	C-25	0.006	0.4	0.15	0.000,364	0.0476	0.008	0.05	947
	R263	C-26	0.008	0.4	0.2	0.000,196	0.0476	0.008	0.05	947
<i>Yan [2008]</i>	R264	e1	0.0144	0.42	0.12	0.0128	0.056,549	0.006	0.06	2000
	R265	e2	0.0232	0.42	0.18	0.0048	0.056,549	0.006	0.06	2000
	R266	e3	0.031	0.42	0.24	0.0022	0.056,549	0.006	0.06	2000
	R267	e4	0.0378	0.42	0.3	0.0012	0.056,549	0.006	0.06	2000
	R268	f1	0.0146	0.42	0.12	0.0072	0.028,274	0.006	0.06	1000
	R269	f2	0.0227	0.42	0.18	0.0031	0.028,274	0.006	0.06	1000
	R270	f3	0.0302	0.42	0.24	0.0015	0.028,274	0.006	0.06	1000
	R271	f4	0.0368	0.42	0.3	0.0011	0.028,274	0.006	0.06	1000
	R272	g1	0.0151	0.42	0.12	0.0037	0.014,137	0.006	0.06	500
	R273	g2	0.0227	0.42	0.18	0.0026	0.014,137	0.006	0.06	500
	R274	g3	0.0302	0.42	0.24	0.0011	0.014,137	0.006	0.06	500
	R275	g4	0.0368	0.42	0.3	0.00,065	0.014,137	0.006	0.06	500
<i>Yang [2008]</i>	R276	RH2Q1	0.0075	0.45	0.075	0.00,141	0.004,398	0.002	0.035	1400
	R277	RH2O2	0.0105	0.45	0.075	0.00,269	0.004,398	0.002	0.035	1400

Table A1. (continued)

	No.	Run	Q ($\text{m}^3 \text{s}^{-1}$)	B (m)	H (m)	S	λ	d (m)	h_v (m)	N (m^{-2})
<i>(B) Flexible Vegetation</i>										
<i>Kouwen et al. [1969]</i>	F1	1	0.002,756	0.61	0.1506	0.0005	0.098,175	0.005	0.1	5000
	F2	2	0.016,956	0.61	0.2527	0.001	0.098,175	0.005	0.1	5000
	F3	3	0.085,496	0.61	0.3819	0.003	0.098,175	0.005	0.085	5000
	F4	4	0.009,081	0.61	0.1519	0.005	0.098,175	0.005	0.1	5000
	F5	7	0.013,163	0.61	0.1509	0.01	0.098,175	0.005	0.1	5000
	F6	8	0.082,736	0.61	0.2422	0.0094	0.098,175	0.005	0.05	5000
	F7	9	0.043,805	0.61	0.3503	0.001	0.098,175	0.005	0.1	5000
	F8	10	0.04,087	0.61	0.25	0.0049	0.098,175	0.005	0.1	5000
	F9	11	0.038,064	0.61	0.4	0.0005	0.098,175	0.005	0.1	5000
	F10	12	0.019,398	0.61	0.3	0.0005	0.098,175	0.005	0.1	5000
	F11	13	0.006,479	0.61	0.1496	0.003	0.098,175	0.005	0.1	5000
	F12	14	0.006,717	0.61	0.2002	0.0005	0.098,175	0.005	0.1	5000
	F13	15	0.049,593	0.61	0.3	0.003	0.098,175	0.005	0.095	5000
	F14	16	0.009,643	0.61	0.2001	0.001	0.098,175	0.005	0.1	5000
	F15	17	0.047,949	0.61	0.199	0.01	0.098,175	0.005	0.06	5000
	F16	18	0.028,379	0.61	0.3498	0.0005	0.098,175	0.005	0.1	5000
	F17	19	0.073,151	0.61	0.2998	0.005	0.098,175	0.005	0.075	5000
	F18	20	0.028,914	0.61	0.3	0.001	0.098,175	0.005	0.1	5000
	F19	21	0.01,647	0.61	0.2	0.003	0.098,175	0.005	0.1	5000
	F20	22	0.02,257	0.61	0.2	0.005	0.098,175	0.005	0.1	5000
	F21	24	0.113,978	0.61	0.3486	0.005	0.098,175	0.005	0.06	5000
	F22	25	0.05,568	0.61	0.3986	0.001	0.098,175	0.005	0.09	5000
	F23	26	0.01,264	0.61	0.2527	0.0005	0.098,175	0.005	0.1	5000
	F24	27	0.075,324	0.61	0.3508	0.003	0.098,175	0.005	0.09	5000
	F25	28	0.031,014	0.61	0.2594	0.003	0.098,175	0.005	0.1	5000
	F26	29	0.142,281	0.61	0.383	0.0049	0.098,175	0.005	0.055	5000
	F27	30	0.003,729	0.61	0.1491	0.001	0.098,175	0.005	0.1	5000
<i>Dunn et al. [1996]</i>	F28	13	0.179	0.91	0.367,052	0.0036	0.005,449	0.00,635	0.152	172
	F29	14	0.18	0.91	0.231,752	0.0101	0.005,445	0.00,635	0.115	172
	F30	15	0.093	0.91	0.257,085	0.0036	0.005,432	0.00,635	0.132	172
	F31	16	0.179	0.91	0.230,072	0.0036	0.001,366	0.00,635	0.097	43
	F32	17	0.078	0.91	0.278,509	0.0036	0.012,284	0.00,635	0.161	388
	F33	18	0.179	0.91	0.283,482	0.0101	0.012,297	0.00,635	0.121	388
<i>Jarvela [2003]</i>	F34	R4-1	0.04	1.1	0.306	0.0015	0.07,389	0.0028	0.205	12,000
	F35	R4-2	0.1	1.1	0.3084	0.0036	0.07,389	0.0028	0.155	12,000
	F36	R4-3	0.04	1.1	0.4065	0.0005	0.07,389	0.0028	0.23	12,000
	F37	R4-4	0.1	1.1	0.4041	0.0013	0.07,389	0.0028	0.19	12,000
	F38	R4-5	0.143	1.1	0.407	0.002	0.07,389	0.0028	0.16	12,000
	F39	R4-6	0.04	1.1	0.5044	0.0002	0.07,389	0.0028	0.245	12,000
	F40	R4-7	0.1	1.1	0.495	0.0006	0.07,389	0.0028	0.22	12,000
	F41	R4-8	0.1	1.1	0.7065	0.0002	0.07,389	0.0028	0.26	12,000
	F42	R4-9	0.143	1.1	0.7037	0.0003	0.07,389	0.0028	0.215	12,000
	F43	S3-1	0.04	1.1	0.4003	0.0004	0.003,619	0.003	0.295	512
	F44	S3-2	0.1	1.1	0.3961	0.001	0.003,619	0.003	0.2	512
	F45	S3-3	0.143	1.1	0.3942	0.0018	0.003,619	0.003	0.17	512
<i>Yang [2008]</i>	F46	FH1Q1	0.0075	0.45	0.055	0.00,361	0.004,398	0.002	0.0226	1400
	F47	FH2Q1	0.0075	0.45	0.075	0.00,151	0.004,398	0.002	0.0275	1400
	F48	FH2Q2	0.0105	0.45	0.075	0.00,266	0.004,398	0.002	0.0253	1400
	F49	FH3Q1	0.0075	0.45	0.11	0.0007	0.004,398	0.002	0.0339	1400
	F50	FH3Q2	0.0105	0.45	0.11	0.00,079	0.004,398	0.002	0.0309	1400
<i>Kubrak et al. [2008]</i>	F51	1.1.1	0.0433	0.58	0.2661	0.0087	0.005,346	0.000,825	0.163	10,000
	F52	1.1.2	0.0384	0.58	0.2576	0.0087	0.005,346	0.000,825	0.163	10,000
	F53	1.1.3	0.0333	0.58	0.2475	0.0087	0.005,346	0.000,825	0.164	10,000
	F54	1.1.4	0.0274	0.58	0.2275	0.0087	0.005,346	0.000,825	0.164	10,000
	F55	1.2.1	0.0422	0.58	0.2236	0.0174	0.005,346	0.000,825	0.161	10,000
	F56	1.2.2	0.0385	0.58	0.2184	0.0174	0.005,346	0.000,825	0.162	10,000
	F57	1.2.3	0.0333	0.58	0.2068	0.0174	0.005,346	0.000,825	0.161	10,000
	F58	1.2.4	0.0274	0.58	0.1951	0.0174	0.005,346	0.000,825	0.162	10,000
	F59	2.1.1	0.0525	0.58	0.2386	0.0087	0.001,336	0.000,825	0.153	2500
	F60	2.1.2	0.0425	0.58	0.2136	0.0087	0.001,336	0.000,825	0.154	2500
	F61	2.1.3	0.0332	0.58	0.1935	0.0087	0.001,336	0.000,825	0.155	2500
	F62	2.2.1	0.0751	0.58	0.2131	0.0174	0.001,336	0.000,825	0.132	2500
	F63	2.2.2	0.065	0.58	0.1925	0.0174	0.001,336	0.000,825	0.131	2500
	F64	2.2.3	0.0547	0.58	0.1799	0.0174	0.001,336	0.000,825	0.133	2500
	F65	3.1.1	0.0605	0.58	0.2386	0.0087	0.001,336	0.000,825	0.151	2500
	F66	3.1.2	0.0504	0.58	0.2234	0.0087	0.001,336	0.000,825	0.152	2500
	F67	3.1.3	0.0408	0.58	0.2005	0.0087	0.001,336	0.000,825	0.153	2500
	F68	3.2.1	0.0693	0.58	0.1962	0.0174	0.001,336	0.000,825	0.132	2500
	F69	3.2.2	0.0555	0.58	0.1876	0.0174	0.001,336	0.000,825	0.139	2500

Table A1. (continued)

	No.	Run	Q ($\text{m}^3 \text{s}^{-1}$)	B (m)	H (m)	S	λ	d (m)	h_v (m)	N (m^{-2})
	F70	4.1.1	0.0609	0.58	0.2421	0.0087	0.001,336	0.000,825	0.151	2500
	F71	4.1.2	0.05	0.58	0.2246	0.0087	0.001,336	0.000,825	0.153	2500
	F72	4.1.3	0.0408	0.58	0.2053	0.0087	0.001,336	0.000,825	0.156	2500
	F73	4.2.1	0.0693	0.58	0.2077	0.0174	0.001,336	0.000,825	0.138	2500
	F74	4.2.2	0.0466	0.58	0.1932	0.0174	0.001,336	0.000,825	0.142	2500
	F75	4.2.3	0.0553	0.58	0.1806	0.0174	0.001,336	0.000,825	0.143	2500
Okamoto and Nezu [2010]	F76	L1.1	0.021	0.4	0.15	0.002,409	0.0478	0.008	0.03	951
	F77	L1.2	0.018	0.4	0.15	0.002,211	0.0478	0.008	0.034	951
	F78	L1.3	0.015	0.4	0.15	0.001,996	0.0478	0.008	0.036	951
	F79	L1.4	0.012	0.4	0.15	0.001,646	0.0478	0.008	0.04	951
	F80	L1.5	0.0102	0.4	0.15	0.001,414	0.0478	0.008	0.042	951
	F81	L1.6	0.009	0.4	0.15	0.001,127	0.0478	0.008	0.044	951
	F82	L1.7	0.0072	0.4	0.15	0.000,775	0.0478	0.008	0.046	951
	F83	L1.8	0.006	0.4	0.15	0.000,56	0.0478	0.008	0.049	951
	F84	L2.1	0.0294	0.4	0.21	0.001,489	0.0478	0.008	0.04	951
	F85	L2.2	0.0252	0.4	0.21	0.001,366	0.0478	0.008	0.045	951
	F86	L2.3	0.021	0.4	0.21	0.001,287	0.0478	0.008	0.051	951
	F87	L2.4	0.0168	0.4	0.21	0.001,058	0.0478	0.008	0.056	951
	F88	L2.5	0.0143	0.4	0.21	0.000,864	0.0478	0.008	0.058	951
	F89	L2.6	0.0126	0.4	0.21	0.000,737	0.0478	0.008	0.06	951
	F90	L2.7	0.0101	0.4	0.21	0.000,505	0.0478	0.008	0.063	951
	F91	L2.8	0.0084	0.4	0.21	0.000,382	0.0478	0.008	0.068	951
	F92	L3.1	0.027	0.4	0.27	0.000,623	0.0478	0.008	0.054	951
	F93	L3.2	0.0216	0.4	0.27	0.000,541	0.0478	0.008	0.06	951
	F94	L3.3	0.0184	0.4	0.27	0.000,486	0.0478	0.008	0.065	951
	F95	L3.4	0.0162	0.4	0.27	0.000,439	0.0478	0.008	0.071	951
	F96	L3.5	0.013	0.4	0.27	0.000,333	0.0478	0.008	0.075	951
	F97	L3.6	0.0108	0.4	0.27	0.000,238	0.0478	0.008	0.078	951
	F98	L4.1	0.0315	0.4	0.315	0.000,041	0.0478	0.008	0.064	951
	F99	L4.2	0.0252	0.4	0.315	0.000,039	0.0478	0.008	0.068	951
	F100	L4.3	0.0214	0.4	0.315	0.000,376	0.0478	0.008	0.076	951
	F101	L4.4	0.0189	0.4	0.315	0.000,331	0.0478	0.008	0.081	951
	F102	L4.5	0.0151	0.4	0.315	0.000,249	0.0478	0.008	0.084	951
	F103	L4.6	0.0126	0.4	0.315	0.000,019	0.0478	0.008	0.096	951

[47] **Acknowledgments.** The writer gratefully acknowledges the help rendered by Hung Tao Shen, Department of Civil and Environmental Engineering, Clarkston University for sharing his experimental data, and also the support from DHI-NTU Centre, Nanyang Technological University, Singapore for this study.

References

- Baptist, M. J. (2005), Modelling floodplain biogeomorphology, Ph.D. Thesis, Delft Univ. of Technol., Delft, Netherlands.
- Baptist, M. J., V. Babovic, J. R. Uthurburu, M. Keijzer, R. E. Uittenboogaard, A. Mynett, and A. Verwey (2007), On inducing equations for vegetation resistance, *J. Hydraul. Res.*, 45(4), 435–450.
- Cheng, N. S. (2003), Application of Ergun equation to computation of critical shear velocity subject to seepage, *J. Irrig. Drain. Eng.*, 129(4), 278–283.
- Cheng, N. S., and H. T. Nguyen (2011), Hydraulic radius for evaluating resistance induced by simulated emergent vegetation in open channel flows, *J. Hydraul. Eng.*, doi:10.1061/(ASCE)HY.1943-7900.0000377, in press.
- Cheng, N. S., Z. Y. Hao, and S. K. Tan (2008), Comparison of quadratic and power law for nonlinear flow through porous media, *Exp. Therm. Fluid Sci.*, 32(8), 1538–1547.
- Dunn, C., F. Lopez, and M. Garcia (1996), Mean flow and turbulence in a laboratory channel with simulated vegetation, Hydrosystem Lab., Univ. of Ill., Urbana, Ill.
- Gioia, G., and F. A. Bombardelli (2002), Scaling and similarity in rough channel flows, *Phys. Rev. Lett.*, 88(1), 1–4, doi:10.1103/PhysRevLett.1188.014501.
- Huthoff, F., D. C. M. Augustijn, and S. J. M. H. Hulscher (2007), Analytical solution of the depth-averaged flow velocity in case of submerged rigid cylindrical vegetation, *Water Resour. Res.*, 43(6), W06413, doi:10.1029/2006WR005625.
- Jarvela, J. (2003), Influence of vegetation on flow structure in floodplains and wetlands, paper presented at Proceedings of the 3rd IAHR Symposium on River, Coastal and Estuarine Morphodynamics (RCEM 2003), Universidad Politecnica de Catalunya, Madrid.
- Kouwen, N., T. E. Unny, and H. M. Hill (1969), Flow retardance in vegetated channels, *Journal of Irrigation and Drainage Division-ASCE* 95(IR2), 329–342.
- Kubrak, E., J. Kubrak, and P. M. Rowinski (2008), Vertical velocity distributions through and above submerged, flexible vegetation, *Hydrol. Sci. J.*, 53(4), 905–920.
- Liu, D., P. Diplas, J. D. Fairbanks, and C. C. Hodges (2008), An experimental study of flow through rigid vegetation, *J. Geophys. Res.*, 113(F4), F04015, doi:10.1029/2008JF001042.
- Meijer, D. G., and E. H. van Velzen (1999), Prototype-scale flume experiments on hydraulic roughness of submerged vegetation, paper presented at XXVIII IAHR Conference, Technical University of Graz, Graz, Austria.
- Murphy, E., M. Ghisalberti, and H. Nepf (2007), Model and laboratory study of dispersion in flows with submerged vegetation, *Water Resour. Res.*, 43(5), W05438, doi:10.1029/2006WR005229.
- Nepf, H. M., and E. R. Vivoni (2000), Flow structure in depth-limited, vegetated flow, *J. Geophys. Res.*, 105(C12), 28,547–28,557, doi:10.1029/2000JC900145.
- Nezu, I., and M. Sanjou (2008), Turbulence structure and coherent motion in vegetated canopy open-channel flows, *J. Hydro-Environ. Res.*, 2(2), 62–90.
- Nikuradse, J. (1933), Stromungsgesetze in rauhen Rohren, Forschung auf dem Gebiete des Ingenieurwesens (in German), Forschungsheft 361, VDI Verlag, Berlin, Germany (English translation: Laws of flow in rough pipes, NACA TM 1292, 1950).
- Okamoto, T., and I. Nezu (2010), Flow resistance law in open-channel flows with rigid and flexible vegetation, in *River Flow 2010*, edited by A. Dittrich et al., pp. 261–268, Bundesanstalt für Wasserbau, Karlsruhe, Germany.
- Poggi, D., A. Porporato, L. Ridolfi, J. D. Albertson, and G. G. Katul (2004), The effect of vegetation density on canopy sub-layer turbulence, *Bound. Layer Meteorol.*, 111(3), 565–587.
- Shimizu, Y., T. Tsujimoto, H. Nakagawa, and T. Kitamura (1991), Experimental study on flow over rigid vegetation simulated by cylindrical with equi-spacing (in Japanese), *Proc. Jpn Soc. Civ. Eng.*, 438/II-17, 31–40.

- Stone, B. M. (1997), Hydraulics of flow in vegetated channels, Master thesis, Clarkson University, Potsdam, New York, U.S.A.
- Stone, B. M., and H. T. Shen (2002), Hydraulic resistance of flow in channels with cylindrical roughness, *J. Hydraul. Eng.*, 128(5), 500–506.
- Vanoni, V. A., and N. H. Brooks (1957), Laboratory studies of the roughness and suspended load of alluvial streams, 121 pp, Sed. Lab., Calif. Inst. of Technol., Pasadena, California, U.S.A.
- Yan, J. (2008), Experimental study of flow resistance and turbulence characteristics of open channel flow with vegetation, Ph.D. thesis, Hohai University, Hohai, China.
- Yang, W. (2008), Experimental study of turbulent open-channel flows with submerged vegetation, Ph.D. thesis, Yonsei University, Korea.
- Yang, W., and S. U. Choi (2010), A two-layer approach for depth-limited open-channel flows with submerged vegetation, *J. Hydraul. Res.*, 48(4), 466–475.

N.-S. Cheng, School of Civil and Environmental Engineering, Nanyang Technological University, Singapore, 639798, Singapore. (cnscheng@ntu.edu.sg)